

AD 603818

RADC-TDR-64-204
Final Report

NANOSECOND-PULSE BREAKDOWN STUDY
AT MICROWAVE FREQUENCIES



TECHNICAL DOCUMENTARY REPORT NO. RADC-TDR-64-204

July 1964

Techniques Branch
Rome Air Development Center
Research and Technology Division
Air Force Systems Command
Griffiss Air Force Base, New York

Project No. 4506 , Task No. 450603

(Prepared under Contract No. AF 30(602)-2782 by Microwave Associates,
Inc., Burlington, Massachusetts, Authors: C. Buntschuh and Dr. M.
Gilden.)

50P

When US Government drawings, specifications, or other data are used for any purpose other than a definitely related government procurement operation, the government thereby incurs no responsibility nor any obligation whatsoever; and the fact that the government may have formulated, furnished, or in any way supplied the said drawings, specifications, or other data is not to be regarded by implication or otherwise, as in any manner licensing the holder or any other person or corporation, or conveying any rights or permission to manufacture, use, or sell any patented invention that may in any way be related thereto.

Qualified requesters may obtain copies from Defense Documentation Center.

Defense Documentation Center release to Office of Technical Services is authorized.

Do not return this copy. Retain or destroy.

Key words: Pulse compression; gas discharges; electric discharges; dielectric properties.

ABSTRACT

Microwave breakdown of gases was studied under short-pulse conditions. An experimental technique was developed for generating and measuring high-power 10 nanosecond pulses at X-band frequencies. Breakdown times were in the range of 2 to 10 nanoseconds and values of E/p extended to 10^4 volts/cm-torr. Normalized breakdown curves for air, nitrogen, helium, Freon 12, SF_6 , Freon C318 and Freon 114 were obtained and compared to theoretical estimates. The agreement was good. Comparison of these results with published breakdown data obtained with nanosecond video pulses enabled values of electron collision frequency to be calculated for air, helium and nitrogen at large values of E/p . For electron attaching gases it was found that some mechanism provided initial ionization and also effected the breakdown threshold.

PUBLICATION REVIEW

This report has been reviewed and is approved. For further technical information on this project, contact AIC R.C. Blackall, RADG (EMATP) Ext 23200.

Approved: *Ronald C. Blackall*
RONALD C. BLACKALL
AIC, USAF
Project Engineer

Approved: *Thomas S. Bond, Jr.*
THOMAS S. BOND, JR.
Colonel, USAF
Chf, Surveillance & Control Division

FOR THE COMMANDER:

Irving J. Gabelman
IRVING J. GABELMAN
Chief, Advanced Studies Group

Evaluation

1. This work is part of an RADC program aimed at utilizing nanosecond pulses to provide superior range resolution in long range radar. Interest has been confined to pulse durations shorter than 20 nanoseconds, which corresponds to range resolution better than 10 feet, and peak powers in excess of 1000 megawatts. The objective of this contract was to gather useful microwave nanosecond pulse breakdown data on selected gases that might be used in such a radar transmitter.
2. The generator developed for the breakdown study used a spark gap switch to release the microwave energy stored in a section of waveguide. This technique produced 300 kilowatt, 11 nanosecond pulses with a rise time less than 1 nanosecond. The time required for a gas to break down was indicated by a distortion of the "flat" portion of the pulse. Any pulse shorter than this time should be transmitted undistorted under the same conditions of power and pressure. The gases tested using this method were air, nitrogen, helium, SF₆, Freon 12, Freon C318, Freon 114, moist air, and air with traces of ozone.
3. Complementary work is being done at Braddock, Dunn and McDonald, El Paso, Texas, and at Space Sciences, Inc., Waltham, Mass. Braddock, Dunn and McDonald, under Contract AF30(602)-2781 entitled "Nanosecond Pulse Breakdown Initiation and Growth," is studying breakdown initiation and the effects of surface conditions on breakdown. Space Sciences, Inc., under Contract AF30(602)-2779 entitled "Nanosecond Pulse Breakdown Study," is investigating nanosecond video pulse breakdown and conditions in the atmosphere that may lead to breakdown of the air under high power pulse conditions.

Ronald C. Blackall
RONALD C. BLACKALL
A1C, USAF
Project Engineer

TABLE OF CONTENTS

	<u>Page No.</u>
I. INTRODUCTION.....	1
II. EXPERIMENTAL APPARATUS AND PROCEDURES.....	4
Pulse Generator.....	4
High Pressure Switch.....	5
Characteristics of the 1' Nanosecond Pulse.....	7
Breakdown Chambers.....	8
Measurement Techniques.....	10
III. RESULTS.....	13
Review of Theory.....	13
Normalized Breakdown Curves.....	15
Additional Experimental Observations.....	16
Minimum Breakdown Time.....	17
IV. DISCUSSION OF RESULTS.....	18
V. SUMMARY AND RECOMMENDATIONS.....	21
REFERENCES	24

LIST OF ILLUSTRATIONS

Figure	Page
1. Block Diagram of Circuit Used in Nanosecond Breakdown Study	25
2. Standing Wave Resonator.....	26
3. Gain and Efficiency Characteristics of the Nanosecond Pulse Generator..	27
4. Transverse Section Through Switch and Waveguide.....	28
5. Output of Nanosecond Pulse Generator (11 ns Pulse).....	29
6. Breakdown Chambers.....	30
7. Low Level Calibration Pulse.....	31
8. Examples of Pulse Distortion by Breakdown.....	32
9. Normalized Pulse Breakdown in Nitrogen.....	33
10. Normalized Pulse Breakdown in Helium.....	34
11. Normalized Pulse Breakdown in Air.....	35
12. Normalized Pulse Breakdown in Water-Air and Ozone-Air Mixture.....	36
13. Normalized Pulse Breakdown in Sulphur Hexafluoride.....	37
14. Normalized Pulse Breakdown in Freon 12.....	38
15. Normalized Pulse Breakdown in Freon C-318.....	39
16. Normalized Pulse Breakdown in Freon 114.....	40
17. Comparison of Normalized Breakdown Curves for Various Cases.....	41
18. Electron Collision Frequency in Air.....	42
19. Electron Collision Frequency in Nitrogen.....	43
20. Electron Collision Frequency in Helium.....	44

I. INTRODUCTION

The study of the breakdown of gases during very short pulses of high power microwave energy was continued with experimental work and correlation of results with basic information derived from other work. The relationship between short pulse breakdown and basic parameters based upon work by Gould and Roberts¹ was discussed in the preceding report². It was pointed out that important parameters were not known, particularly for the large values of E/p encountered in nano-second duration breakdown. It was also shown theoretically how the breakdown time would be a function of the size of the region of initial ionization. Therefore, an experimental evaluation was recommended and it was concluded that it would be feasible to make short pulse breakdown studies in gases. This required the design and construction of equipment to generate short, high-power pulses at microwave frequencies. The apparatus is similar to, but simpler than one recently described by Swartzkopf³.

Related to this work are the breakdown measurements using video pulses, carried out concurrently by Proud and Felsenthal⁴. Their measurements have shown a good agreement with theoretical predictions when conditions are chosen in which electron paths are short enough to avoid collisions with the walls during an electron avalanche. However, one additional factor, the ratio between the effective and the rms value of RF field, is still required to correlate microwave breakdown with such experimental results. Direct microwave measurements

of short pulse breakdown in hydrogen have been made by Cottingham and Buchsbaum⁵; they were able to show close agreement with theory by assuming that the electron collision frequency at breakdown is proportional to gas pressure. Earlier work on short-pulse microwave breakdown in connection with the spike leakage of TR tubes was carried out by Christoffers, Dougal and Goldstein⁶. A particularly interesting result was that for a constant power level there is a minimum breakdown time as pressure is varied at constant power. In general the minimum breakdown time decreases with increasing field strength. The probability of initial ionization or electrons being present for breakdown have been discussed by McDonald and Brient⁷.

The motivation for this work stemmed from the interest in developing high resolution radar systems using nanosecond pulses. Inasmuch as the peak power levels will be well beyond the CW breakdown threshold for the gases in the system, the question arose as to whether a greatly reduced pulse length would, in fact, prevent breakdown from occurring. The object of this work was to obtain breakdown data from which nanosecond pulse breakdown field strengths can be predicted at microwave frequencies with gases which might be used in radar systems.

The scope of this work included the development of equipment for generating high power nanosecond pulses and for measuring breakdown field strengths and breakdown intervals. The generation technique used a spark gap switch to release the energy stored in a linear resonator. The method of studying the breakdown consisted of measuring the time required for distortion of the pulse by breakdown to occur.

The pulse envelope was displayed on a traveling-wave oscilloscope so that the breakdown time could be measured directly from the trace. The power level was determined by comparison with a low level reference pulse of known amplitude. The gases studied were air, nitrogen, helium, SF₆, Freon 12, Freon C318, Freon 114, moist air, and air with traces of ozone.

The results of our experiments and analysis confirmed that basic parameters determined by standard techniques^a can be used to predict microwave breakdown. The results showed also that the high dielectric strength gases are better than air at the short pulse lengths, even though extrapolated values of the first Townsend coefficients suggested that this might not be so^b. In the course of the experiments several other effects were observed which are significant with respect to failure of microwave systems. Finally, in carrying out the experiments, it was demonstrated that the generation of high power nanosecond pulses of microwave energy for laboratory experiments can be satisfactorily carried out with the apparatus developed in the course of this work.

Section II presents a description of the experimental techniques, the apparatus and the method of treating the data. Section III contains a brief review of the breakdown theory and a presentation of the results of the experiments. Detailed analysis of the breakdown theory was covered in the preceding report². A discussion of the results with explanations of some of the unexpected observations is given in Section IV and in Section V are the conclusions and recommendations.

II. EXPERIMENTAL APPARATUS AND PROCEDURES

Pulse Generator

A major effort in this program was the development of the pulse generator and the instrumentation for determining the breakdown time and pulse amplitude. A block diagram of the apparatus shown in Figure 1 includes three major sections: the pulse generator, the detector circuit, and the breakdown chamber. The various parts of the circuit will be discussed in more detail below.

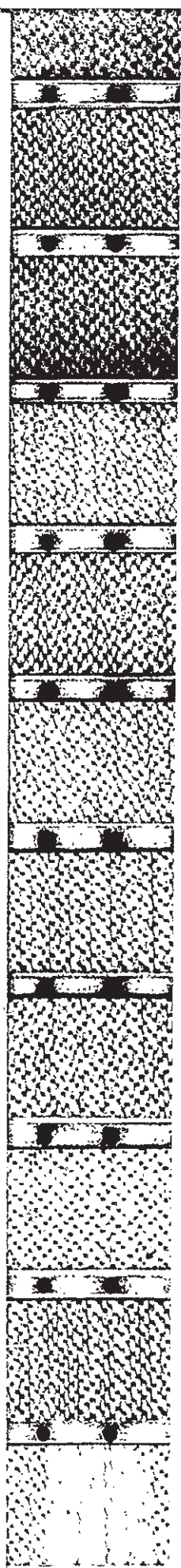
The pulse generator, Figure 2a, consisted of a length of waveguide which was made into a resonator by an input iris at one end and a series open-circuit switching gap at the other end. An equivalent circuit for the resonator is shown in Figure 2b emphasizing the use of the transformers, the condition for resonance in terms of electrical length and the resonant nature of the open-circuit gap. A standing wave was set up in the resonator in which the peak power of the two components of the standing wave was well in excess of the peak power in the incident wave. The resonator in Figure 1 was preceded by a waveguide power divider to control the power level and this in turn was preceded by a circulator. The primary source was an X-band magnetron which provides up to 200 kilowatts of peak power in a pulse length of one microsecond. The repetition rate of the transmitter was variable from approximately 50 to 1500 cycles per second. The frequency of operation was set at 9 Gc. The waveguide components were made of WR 112 waveguide to reduce waveguide losses.

The mode of operation of the pulse generator consisted of charging up the resonator with the microsecond pulse. The charging time is much shorter than a microsecond. At some time after the resonator was charged, the trigger discharge was fired. This in turn initiated an arc across the switching gap which essentially closed the switch. The standing wave components then moved out of the resonator in a pulse whose physical length was twice that of the resonator and whose temporal length was twice the cavity length divided by the group velocity. The length of the resonator section used yielded a pulse length of 11 nanoseconds.

The range of efficiency of the pulse generator and the power gain relative to the input power for critical coupling are shown in Figure 3 as functions of the ratio of the charging time to the output pulse length. The lines of constant efficiency sketched in the figure show that the optimum efficiency would be slightly less than 50 percent. This optimum point of operation corresponds to the generator releasing its energy somewhat before it becomes fully charged. If the generator is allowed to remain in the charged state for a longer period of time, the overall efficiency would drop rapidly. For purposes of studying breakdown only the power gain was important. Its relationship to values of input coupling for critical coupling are shown by the right hand ordinate in Figure 3.

High Pressure Switch

The switch was the key item in the pulse generator. It was required to hold off extremely high field strengths until triggered, and



after triggering, to allow formation of a high pressure discharge in about a nanosecond. The switch sketched in Figure 2 and detailed in Figure 4, consisted of a resonant gap in the top wall of a reduced height section of waveguide. The plate containing the gap was removable. The gap was coupled to a tunable cavity which was approximately a quarter wavelength long at the frequency of operation. Thus the gap presented a series open-circuit in the waveguide. In operation the switch provided an isolation greater than 30 db, indicating that its losses were small even though the structure was demountable. Illumination of the switch gap by the trigger discharge - illustrated by the dashed line in Figure 4 - caused an arc to form in the presence of the microwave field, thus shorting out the series open circuit. The trigger gap was an automobile spark plug with the points modified so that efficient illumination of the switch gap was obtained. The purpose of transforming to the reduced height section was to obtain the best hold-off power and also to obtain large current flows across the gap. The thought was that the arc loss would be minimal under these conditions. For a given gap size and power level, the voltage across the gap is proportional to the square root of the waveguide impedance. Therefore, as low an impedance as possible was desirable for best hold-off. In practice however the waveguide height was made slightly larger than the gap to make the fields in the gap slightly larger than that in the waveguide. This prevented the waveguide from breaking down before the gap. Typically the gap was .060 inches and the waveguide height 0.100 inches.

Characteristics of the 11 Nanosecond Pulse

A typical wave form of the pulse generated is shown in Figure 5. This is an enlargement of a photograph of a signal as displayed on a traveling-wave deflection oscilloscope (Manufactured by EG&G). Time runs from right to left. The signal was obtained from a specially designed broadband detector which could provide the nominal 3 volt signal level required for adequate deflection. A high voltage MA 462 diode was used. The second step following the main pulse is due to a reflection from the "closed" switch which has traveled to the input iris and back. Had the switch operated without loss, this step would have disappeared. The relative amplitudes of the main pulse and the first reflection are deceiving because the broadband detector was, of necessity, operating close to saturation with the result that the ratio of the two amplitudes is greater than indicated in the figure. The shape of the pulse has an initial rise in amplitude which is approximately a nanosecond in duration followed by a slowly rising amplitude throughout the remainder of the pulse. The rapid rise appears to be due to one mechanism while the much slower adjustment of the arc during the remainder of the pulse appears to be due to a second mechanism. Measurements of the arc loss based on the input power charging the resonator and the output pulse wave shape indicated that the insertion loss of the switch was approximately 3 db; a value considerably higher than had been anticipated at the outset of the experiments. The variation between the leading and trailing edge of the pulse as measured with a reference pulse was found to be as large as 4 db in some cases.

The reduction of the breakdown data therefore required this variation to be taken into account.

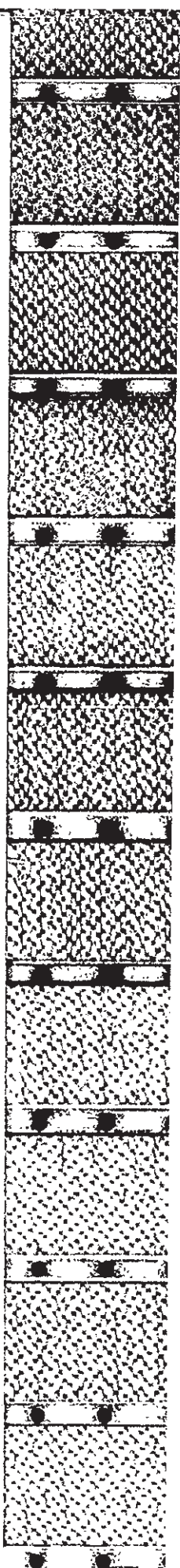
The pulse generator had other interesting characteristics. The trigger discharge illuminating the gap could be operated over as much as a 5:1 dynamic range of input power while still giving a well shaped output pulse. At the lower power levels the corners of the pulse became more rounded. When the power level was close to the upper limit, it was found that the switch would frequently fire spontaneously in advance of the trigger discharge. It was observed that the spontaneous pulses frequently had a good shape; however, the time of firing was somewhat erratic. The upper limit of operation was determined primarily by a predominance of the spontaneous pulses and the lower limit by severe rounding of the pulse shape. A flow of gas through the gap reduced the rate of early firing but, if the gas flow rate were too great the pulse became rounded and unstable. Air was the most satisfactory as well as the most convenient gas.

Breakdown Chambers

Two types of breakdown chambers were used in the experiments. One chamber was a straight section of WR 90 waveguide, Figure 6a, for which Parker seal gaskets and the dielectric windows of either Mylar, Teflon or H film were used for sealing. One gas inlet is shown near the input window. A second gas port on the opposite wall, not shown in Figure 6a, leads to the vacuum gauges and pump. Needle valves were included so that a dynamic system could be used. With the valves closed the leak rate was low and a mechanical pump could reduce the

system pressure to less than 20 microns. A second breakdown chamber was the reduced height section shown in Figure 6b. This chamber consisted of a step transformer to a reduced height section one-fifth the height of the waveguide (i.e., .080 inches in WR 90 waveguide). Inductive irises were added in the reduced height section to form a low Q cavity; the field strength in this section was 5.8 times that in the full height waveguide. It was determined that the pulse was not appreciably distorted by the transformer or the low Q resonator. Figure 7 shows the change of wave shape of the low level reference pulse after passing through the chamber. The edges of the transformer steps were rounded to prevent breakdown from being initiated inadvertently. At the front iris a mica window was placed to serve as a controlled leak and to confine the breakdown to the reduced height section. A final calibration of the reduced height section was made by breakdown at atmospheric pressure using a microsecond pulse; this determination agreed well with the design value.

The gases were introduced through controlled leaks while pumping continuously through a throttle valve so that a relatively pure gas fill was present during the breakdown experiments. After completion of a set of measurements the inlet valve would be closed and the chamber pumped down before being refilled. The gases used in the experiment were commercial grade and no attempt was made to get a precise determination of the impurities in the gas. The pressure was measured by aneroid manometers, one with the range 0 to 100 Torr and the other with a range from 0 to 800 Torr. The experiments with water vapor



were carried out by using a side tube of water through which air was bubbled as it flowed to the breakdown chamber. The traces of ozone were obtained by flowing gas from the switch into the breakdown chamber; however, a determination of the amount of ozone present was not made. In several experiments a mica baffle was placed in the full height section of waveguide to direct a flow of gas against the dielectric window. The flow rate was varied to ascertain whether or not there would be an influence on the breakdown thresholds.

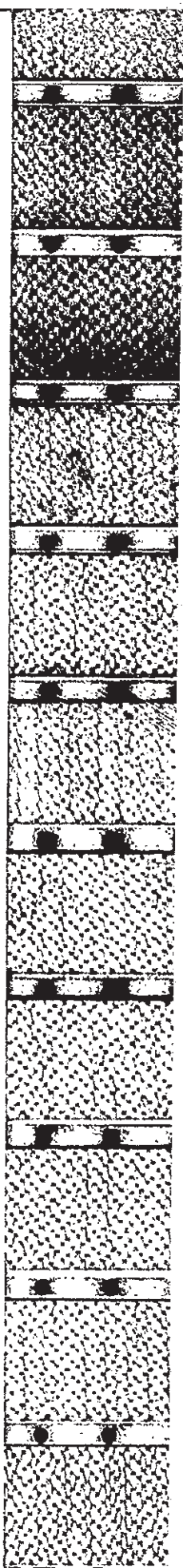
Measurement Techniques

The three quantities measured in the experiment were the breakdown time, the gas pressure, and the peak power. The temporal length of the pulse was calculated from the group velocity and this value was verified by comparison on the oscilloscope with a similar video pulse generated by discharging a known length of cable. The breakdown time was determined by a linear scaling of distances on the face of the oscilloscope tube. Since the sweep of the oscilloscope was linear except for the first 10 percent of the trace, the triggering level was adjusted to place the pulse in the middle of the trace. An estimate of over-all time accuracy was ± 0.5 ns including effects of jitter of the signal.

The peak power was measured by a section of the circuit shown in Figure 1. The circuit allowed a precisely attenuated sample of the high power pulse and a low level reference pulse to be compared simultaneously on the oscilloscope. The pulsed reference signal was obtained from a CW source by using a varactor switch which normally allowed the power to pass on to a power meter. The varactor switch

is pulsed periodically to reflect the power into the detector for intervals of approximately 10 nanoseconds. Since the duty cycle was extremely low (less than 10^{-5}), the power meter measured the CW level of power which, after taking into account the switch losses and other insertion losses, yielded an accurate measurement of the reference pulse amplitude. The high power pulse was attenuated through a calibrated directional coupler and a precision attenuator. The attenuator was adjusted to obtain equal amplitudes of the two pulses on the oscilloscope. The reference pulse was used to measure the amplitude of both the leading and trailing edges of the high power pulse inasmuch as the reference pulse was reasonably flat. The shape of the reference pulse is shown in Figure 7a. The accuracy of determining the pulse amplitude was limited to some extent by the fact that the detector was nonlinear because of the large signal amplitude and also by the fact that when the two pulses appeared together the high power pulse had additional jitter. An amplitude could be measured to within ± 0.25 db.

The experimental procedure consisted of first setting and measuring the power level of the high power pulse and then varying the gas pressure while determining the length of the breakdown time. A steady indication of breakdown time was usually obtained as shown by the breakdown distorted pulses in Figure 8. The point of breakdown is very clearly defined and the breakdown time was taken as the pulse length multiplied by the fractional distance from the leading edge to the breakdown point. It was necessary to account for the fact that the pulse did not have a flat top. An analysis indicated that when the



pulse amplitude was increasing, the appropriate average value of field strength or power is the value at a time half-way between the leading edge of the pulse and the point of breakdown.

III. RESULTS

Review of Theory

The results of our study will be given in this section; however, a brief summary of the theory will be given first. The earlier report³ and the other cited references^{4,5} give a detailed discussion of the pulsed breakdown theory. Under conditions where the parameters controlling breakdown do not change with time during the pulse, the electron density buildup during breakdown is exponential:

$$n = n_0 e^{(\nu_{\text{net}} - D/\Lambda^2)t} \quad (1)$$

where n_0 is the initial electron density, ν_{net} is the net rate of electron production which is a function of E/p , D is the diffusion coefficient for electrons in the gas and Λ is the diffusion length which is related to the gap spacing. The usual breakdown criterion is that the logarithm of the ratio of the final density, n_f , to initial density be some constant value for the breakdown time, τ

$$\log_e n_f/n_0 = \text{constant} = \left(\frac{\nu_{\text{net}}}{p} - \frac{D}{p\Lambda^2} \right) p\tau \quad (2)$$

The quantities on the right hand side of Equation (2) are grouped into the proper normalized variables, ν_{net}/p , D/p , $p\Lambda$ and $p\tau$. Gould and Roberts have recommended that the constant have the value $18.4 = \log_e 10^8$ as a result of curve fitting long-pulse breakdown measurements¹. Examination of the theory further indicates that values

ranging from $\log_e 10^7$ to $\log_e 10^9$ do not cause large variations in the predicted breakdown conditions. There is also a relationship between the rms value of the RF field strength and an equivalent dc value which must be used with the RF breakdown theory¹,

$$\left(\frac{E_{\text{eff}}}{P}\right)_n = \frac{E_{\text{rms}}}{P} \frac{1}{\sqrt{1 + \left(\frac{C}{p\lambda}\right)^2}} + \Delta(p\lambda) \quad (3)$$

where $C/p\lambda = \omega/v_c$ and v_d in the electron collision frequency.

The first term is a correction reflecting the effectiveness of the RF field in heating the electrons and the second term, $\Delta(p\lambda)$, takes into account the fact that, at high pressures, the electron energy is modulated at twice the RF frequency with the peak value of energy corresponding to the peak value of the RF field rather than the rms value. Both correction terms are functions of the quantity $p\lambda$, the product of pressure and free space wavelength. All of the experimental results are presented in terms of E_{rms}/p and $p\tau$ while the theory is presented in terms of $(E_{\text{eff}}/p)_n$ to show where the corrections become necessary.

The data can be reduced, taking the above factors into account, so that comparison can be made with extrapolated theory. For large values of E/p , particularly for the high dielectric strength gases, the parameters are not well known so that it is impossible to reduce the data to $(E_e/p)_n$. The unknown parameters are the mean electron energy, collision frequency, drift velocity and first Townsend coefficient. Therefore, it becomes valuable to have direct measurements of the exponential factors which operate during short pulse breakdown. In view

of the theory for breakdown, it was expeditious to plot the breakdown data first in terms of E_{rms}/p versus p and then attempt to evaluate the correction factors required to obtain the equivalent dc fields.

Normalized Breakdown Curves

Normalized breakdown curves are shown in Figures 9 through 16 for nitrogen, helium, air, air with water vapor and with traces of ozone, SF_6 , Freon 12, Freon C318 and Freon 114. The experimental points are E_{rms}/p while the theoretical curves, where plotted, are $(E_{eff}/p)_n$. For nitrogen, air and helium experimental video pulse data from Proud and Felsenthal⁴ are also included. In general, the shape of the curves are as expected from theoretical considerations. The repetition rates, as indicated, range from 50 pulses per second to 1000 pulses per second. For air, Figure 11, a pronounced lowering of E/p with repetition rate is evident. The values of breakdown time ranged from 2 to 10 ns and the field strengths to values as high as 40,000 volts/cm. The data includes results from the breakdown chamber consisting of a full-height section of WR 90 waveguide and the reduced height section containing the low Q cavity. One disconcerting result was that, although the measurements from the two breakdown chambers agreed well for the non-attaching gas, nitrogen and helium, for the attaching gases there was a marked difference - values of E/p were higher from the reduced height section. In view of electron diffusion being more important for non-attaching gases, just the reverse situation would be expected. This anomaly will be discussed in the next section. In Figure 12, data for air saturated with water and air with traces of ozone showed no significant changes in breakdown threshold.

For comparison purposes, the results were summarized in Figure 17, where curves indicated by number 1 are for the reduced height section and number 2, the full height section. Another observation was that the results from the full height section do not differ greatly from gas to gas as compared to the reduced height section. For reference, lower limit values for E/p for CW breakdown are shown on the right hand scale⁹.

Additional Experimental Observations

Several other observations of breakdown with these short pulses are worth noting. It was found that the reduced height section required the insertion of a window at the iris as shown in Figure 6, in order to obtain reproducible results. Prior to this, the results were inconsistent and could not be correlated with measurements made in the full height waveguide section. Related to this is that in the full height chamber there was evidence that the breakdown was occurring at the window closest to the source. A radio-active source was used in the measurements to initiate the discharge; however, in many of the gases, it was found that once the breakdown was started it would continue from pulse to pulse without the benefit of the radio active source. For the attaching gases where free electrons cannot survive in the interpulse period, these observations indicate that some mechanism other than residual electrons has taken over the role of providing initial electrons for the breakdown. In this connection, experiments with gas flow across the window did not change the breakdown threshold significantly.

Minimum Breakdown Time

A useful result is that for a given power level, there is a minimum breakdown time for a particular pressure. This means that a maximum pulse length can be selected for which breakdown should not occur under any value of pressure. This can be seen very simply by considering a new normalized variable in which pressure does not appear explicitly,

$$(E/p)(p\tau) = E\tau \quad (4)$$

(values can be obtained from the E/p versus $p\tau$ curves). Now, contours of constant values of $E\tau$ can be plotted on the normalized breakdown curves (E/p versus $p\tau$) as straight lines with a slope of -1 on log-log graph paper. The smaller the value of $E\tau$, the further to the left the line is located. Therefore, referring to the short pulse breakdown curve for air, Figure 11, the smallest possible value of $E\tau$ corresponds to that line which is tangent to the steeply rising part of the curve. From this absolute minimum value of $E\tau$, τ_{\min} values can be calculated for given values of E ,

$$\tau_{\min} = \frac{(E\tau)_{\min}}{E} \quad (5)$$

For air, nitrogen and helium the $(E\tau)_{\min}$ values are approximately 8×10^{-6} , 6×10^{-6} and 13×10^{-6} volt-sec/cm respectively.

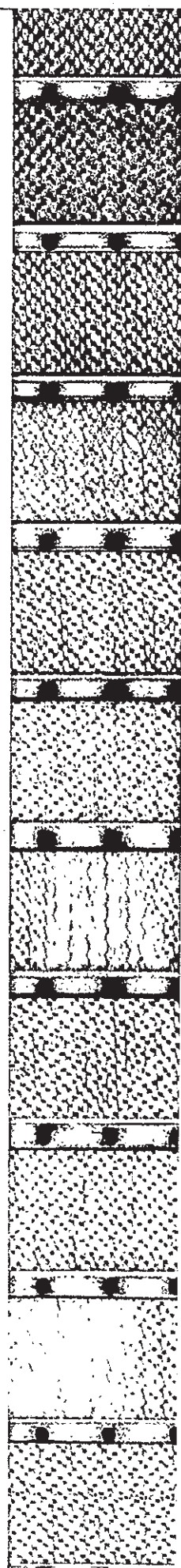
IV. DISCUSSION OF RESULTS

The results of breakdown studies with short pulses can be compared with theory where enough basic information exists. In the work reported here for air, nitrogen and helium there is agreement with theory; in fact, considering the extent of the extrapolation³ one might say the agreement is quite good. The results for SF₆, Freon 12, Freon C318 and Freon 114 could not be compared to an extrapolated theory; however the shapes of the breakdown curves are as expected. The values of E/p are greater for the high dielectric strength gases, than for air therefore they should be valuable in high power short pulse waveguide systems. It was also interesting to note that the presence of water vapor or ozone in air did not cause any significant deviation from the data taken with pure air.

The results for air, nitrogen and helium have been compared with the short video pulse measurements of Proud and Felsenthal⁴. Since they used video pulse techniques, their values of field strengths were effective values. For the microwave measurements at low pressures, the effective fields are related to the rms values by Equation (3) which requires values of electron collision frequency. Therefore, with the two sets of data it is possible to calculate the values of collision frequency at low pressures where the video and microwave data begin to deviate. This was done and the resultant values of ν_c/p were plotted in Figures 18, 19 and 20. For air the results show a definite trend of increasing ν_c/p with increasing values of E/p. The collision frequency increases approximately linearly and the curve includes the

value which was used by Gould and Roberts⁸ for long pulse breakdown where values of E/p are close to the CW breakdown value. The results for nitrogen and helium scattered considerably and it is difficult to determine a trend. Nitrogen appears to have a characteristic similar to air; however, there is insufficient data for larger values of E/p. Helium appears to have a v_c/p with a tendency to decrease with increasing values of E/p. For reference, the value from Brown⁸ for low E/p is also shown. This value appears consistent with the downward trend; however, there is no theoretical basis for the effect.

An interesting effect which deserves more attention is the difference between the breakdown measurements made in the full height chamber and in the reduced height cavity chamber with the attaching gases. In the cavity it was necessary to put a mica window immediately at the entrance to the chamber in order to get reproducible results. In the full height waveguide a dielectric window of teflon or mylar was used as a matter of course to hermetically seal the chamber. There was evidence that breakdown occurred at the window. A possible explanation is that the products of the breakdown of the gas (including positive ions, negative ions and free radicals) interact with the dielectric material or become attached to it in such a manner as to make the breakdown occur consistently at the window itself. The threshold may be lowered somewhat while the actual formation of the discharge is controlled by the pressure of the gas. Similar effects have been found at Microwave Associates in high power duplexer studies where material such as quartz, beryllia and alumina are used as windows



to the chambers containing the gases used for switching. Under identical geometrical conditions while the high power was being switched by the internal discharge, arcing occurs at the external surfaces of the different windows at quite different power levels. Quartz was superior to both alumina and beryllia in this respect. The evaluation of these high power duplexers was done in the presence of attaching gases. The conditions at the surface of the dielectric could be an important factor, because in any very high peak power radar system using nanosecond pulses, there will be radomes or windows somewhere in the system. The question arises whether arcing or discharges can occur at these radomes or windows since the values of E/p will be high enough to cause ionization, if not breakdown.

Another related phenomenon is the disassociation of negative ions in air when E/p exceeds values of 90^{10} . A high density of such negative ions, present before the pulse of energy, could be the major source of electrons for initiating a breakdown. In contrast to free electrons, the negative ions have a much longer life-time so that the density can build up over a number of pulse periods. These negative ions may perhaps be collected on the dielectric surface.

V. SUMMARY AND RECOMMENDATIONS

We have established short-pulse breakdown curves using pulse lengths in the range of 2 to 10 nanoseconds for air, nitrogen, helium, Freon 12, SF₆, Freon C318 and Freon 114. We have also studied air with water vapor and with traces of ozone. The normalized breakdown curves include values of E/p up to values of 10⁴ and values of pr as small as 10⁻⁹. Because of the limit on high power levels, the larger values of E/p correspond to values of pressure in the range of 10 torr. The experimental results do not show any great discrepancies with theoretically predicted breakdown. We have also shown that the microwave pulse breakdown together with video pulse breakdown provide a useful method for determining electron collision frequency at large values of E/p.

The study indicates that an important source of ionization for breakdown is the gradual buildup of charged particles and possibly free radicals due to values of E/p exceeding the CW breakdown threshold. If at some arbitrary time a single electron appeared in the system, ultimately a low density of negative and positive ions and free radicals would be distributed throughout the system. Thus one of our earlier analyses² which predicted a modified breakdown time taking into account the effect of the growth of the region of ionization, does not appear to be as important as was originally thought. Furthermore the source of initial free electrons appears to be less important than the effect of ions and radicals in the presence of dielectric materials used for radomes or microwave windows. These

materials, perhaps by collecting the ions, appear to play an important role in initiating the discharge or at least in insuring that the discharge strikes consistently from pulse to pulse once a certain threshold has been reached. Our experiments indicate that there is a difference in breakdown threshold with the attaching gases when mica and teflon are used. When values of E/p in air exceed a value of 90 it becomes possible for negative ions in air to give up their electrons directly, thus if a high density of negative ions are present, these electrons are released immediately to contribute to the breakdown process.

The technique for generating short high power microwave pulses using energy storage in a resonator and a high pressure spark gap is satisfactory. In the course of the experiments at X-band frequencies peak power levels of 25 to 150 kilowatts were normally used over long periods of time. The largest levels attained were about 300 kilowatts; at that level the resonator itself was holding off about 800 kilowatts when switch loss is taken into account.

The following recommendations are made: 1) more experimental work, at even higher power levels, is necessary, particularly to get data for high values of E/p in the range where the pressures are much higher than obtained in these experiments. 2) It would also be valuable to continue the experiments to obtain better values for the electron collision frequency at high values of E/p by the technique described in the report. 3) The effects of dielectric materials at high values of E/p and other possible long-time effects in a waveguide

system should be explored further as this may turn out to be a serious limiting factor for radar systems using such short pulses of very high peak power.

REFERENCES

1. L. Gould and L. W. Roberts, "Breakdown of Air at Microwave Frequencies," Jour. App. Phy. 27, 1162 (Oct. 1956).
2. C. Buntschuh, B. Salkins and M. Gilden, "Nanosecond Pulse Breakdown Study" Final Report, Microwave Associates, RADC-TDR-63-82 (Rome Air Development Center), February 21, 1963.
3. D. B. Schwarzkopf, "The Traveling-Wave Resonator as a Short Pulse Generator," Microwave Jour. V, 172-180 (Oct. 1962).
4. J. M. Proud and P. Felsenthal (to be published by Rome Air Development Center).
P. Felsenthal, "Nanosecond Breakdown in Gases," Bulletin Amer. Phy. Soc. II-9, 468 (April 1964).
5. W. B. Cottingham and S. J. Buchsbaum, "Electron Ionization Frequency in Hydrogen," Phy. Rev. 130, 1002-1006 (May 1963).
6. W. H. Christoffens, A. A. Dougal and L. Goldstein, "T-R Tube Spike Leakage," Final Report DA-36-039-SC-52670, October 1955.
7. D. F. McDonald and S. J. Brient, "Nanosecond Pulse Breakdown Initiation and Growth," Bradock, Dunn and McDonald, Inc. RADC-TDR-63-525 (Rome Air Development Center), January 1964.
8. S. C. Brown, Basic Data of Plasma Physics, John Wiley and Sons, 1959.
9. M. Gilden, "High Power Capabilities of Waveguide Systems," Final Report, Microwave Associates, NObsr 85190 June 1963.
10. L. B. Loeb, "Recent Developments in Analysis of the Mechanism of Positive and Negative Coronas in Air," Jour. of App. Phy. 19, 882-897 (1948).

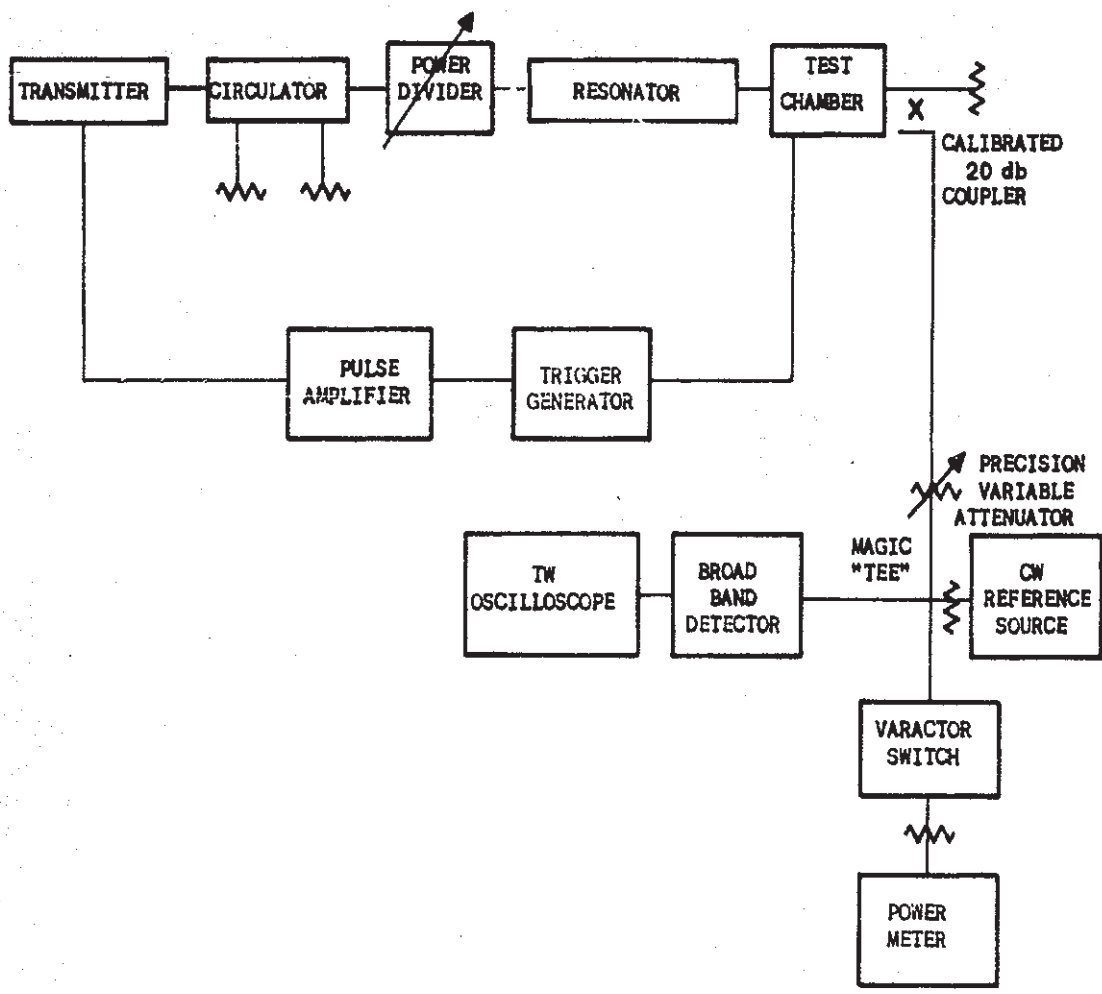
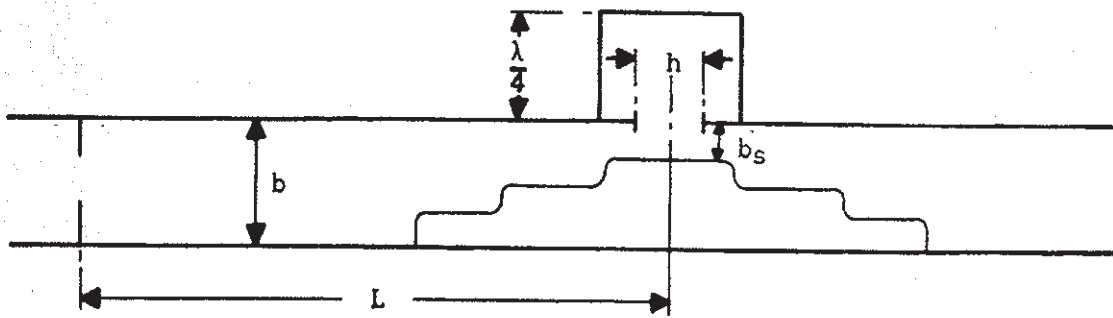
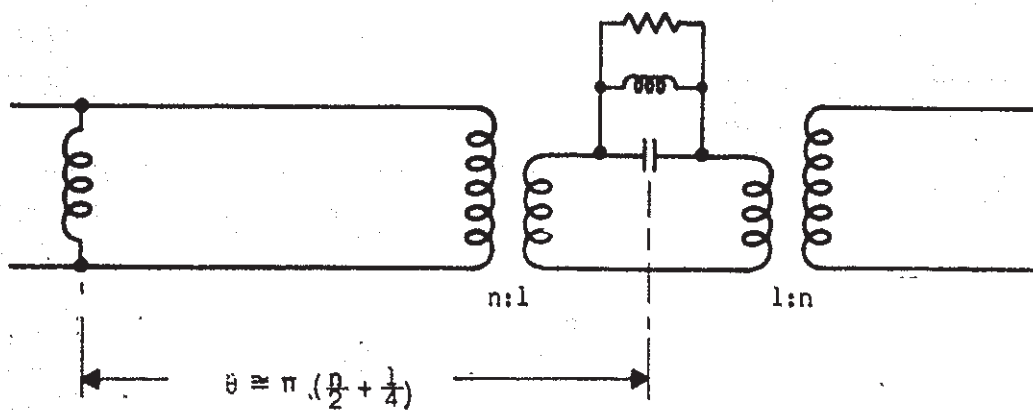


FIGURE 1
 BLOCK DIAGRAM OF CIRCUIT USED IN NANOSECOND BREAKDOWN STUDY

D-1370



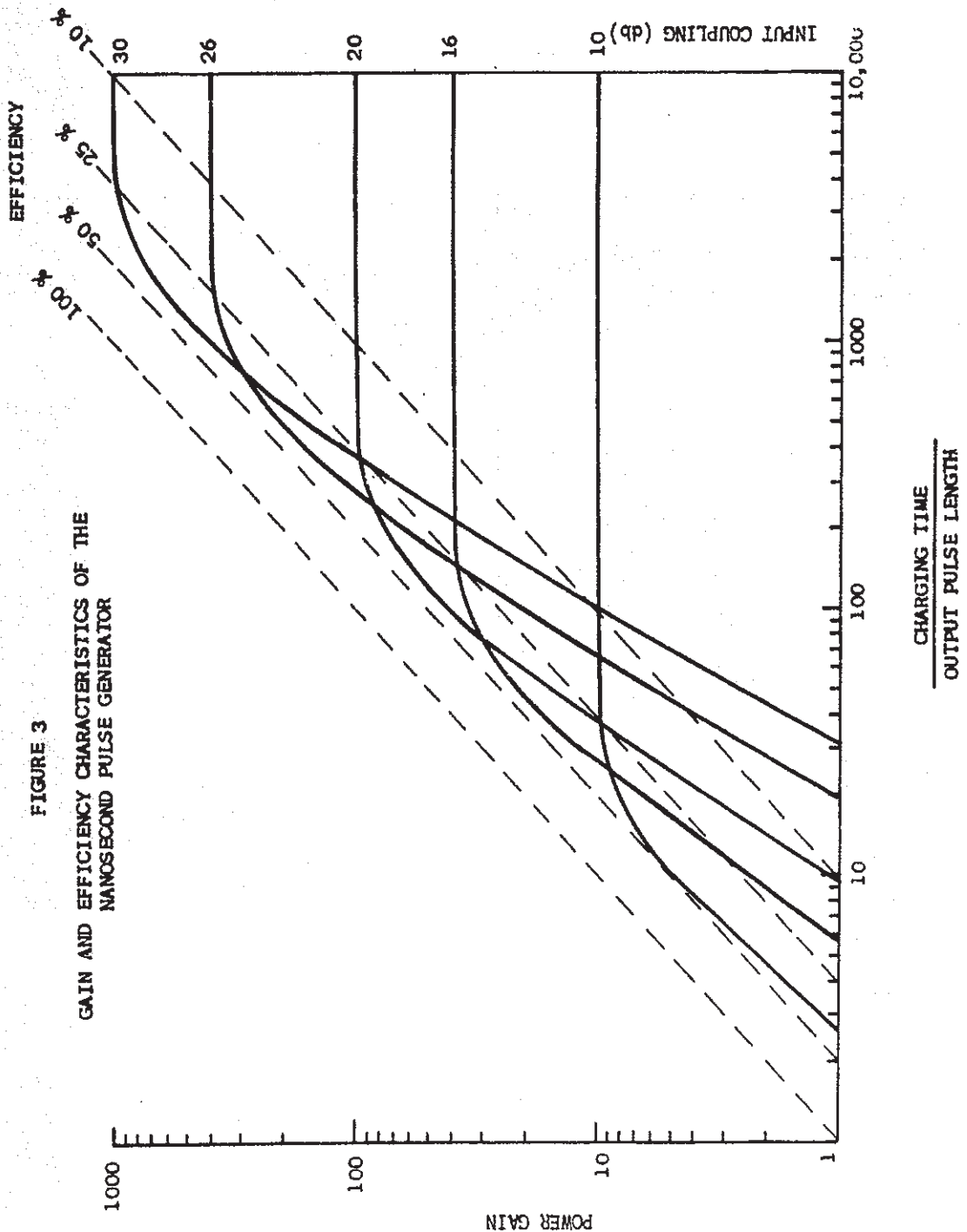
(a.) SIDE VIEW OF WAVEGUIDE



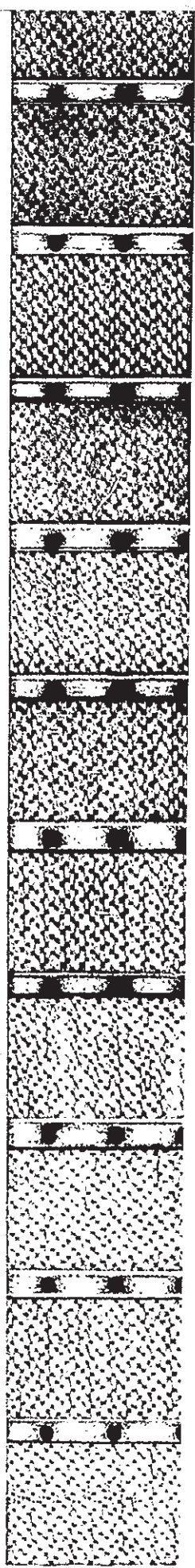
(b.) EQUIVALENT CIRCUIT

FIGURE 2
STANDING WAVE RESONATOR

D-1020



D-1236



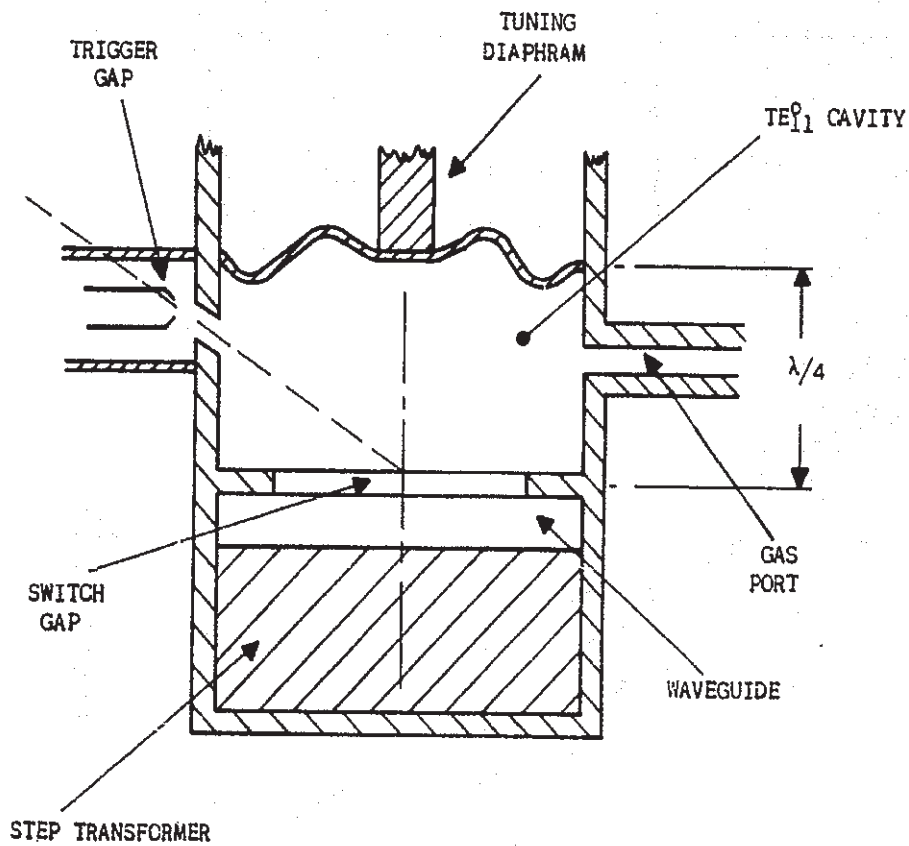


FIGURE 4
 TRANSVERSE SECTION THROUGH SWITCH AND WAVEGUIDE

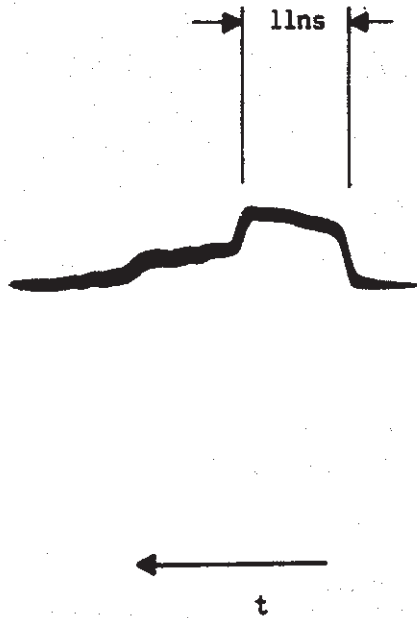
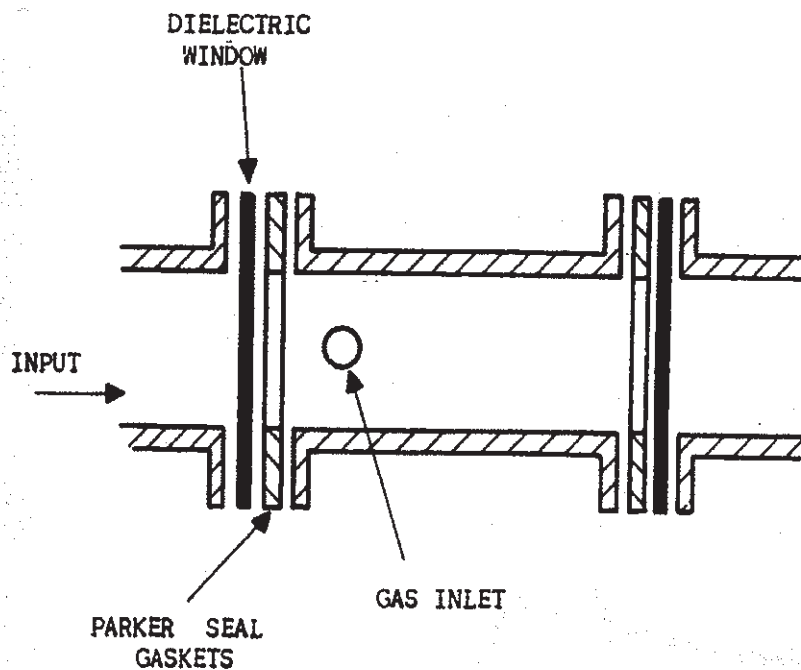
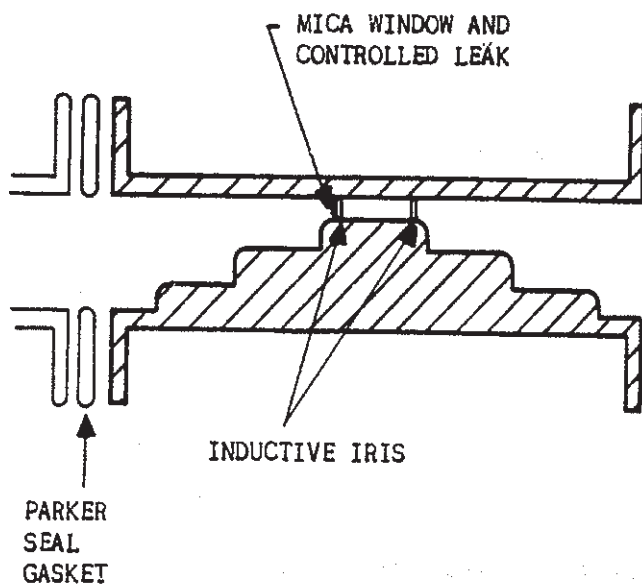


FIGURE 5
OUTPUT OF NANOSECOND PULSE GENERATOR
(11 ns PULSE)

D-1314

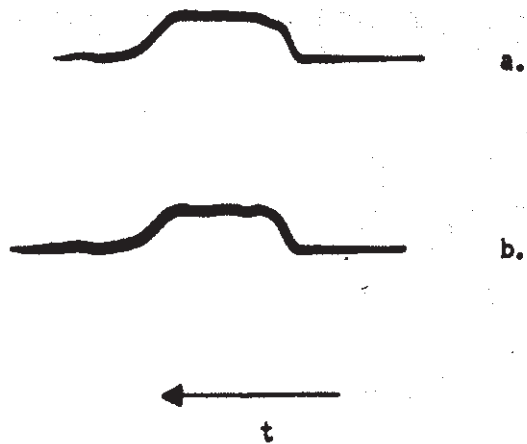


a.) SIDE VIEW OF FULL HEIGHT BREAKDOWN CHAMBER



b.) SIDE VIEW OF REDUCED HEIGHT BREAKDOWN CHAMBER

FIGURE 6
BREAKDOWN CHAMBERS



- a) UNDISTORTED PULSE
- b) PULSE AFTER PASSAGE THROUGH BREAKDOWN CAVITY

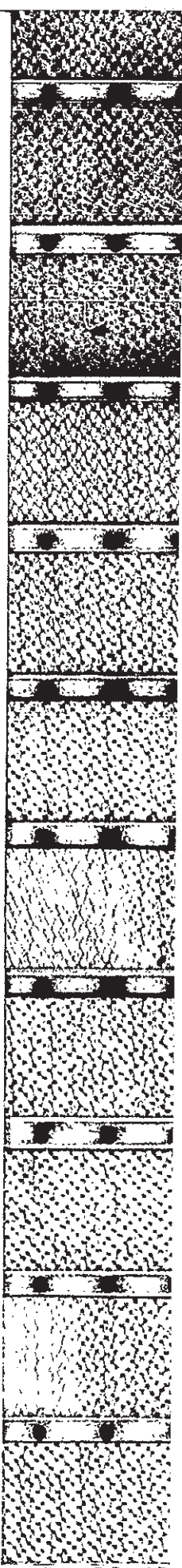
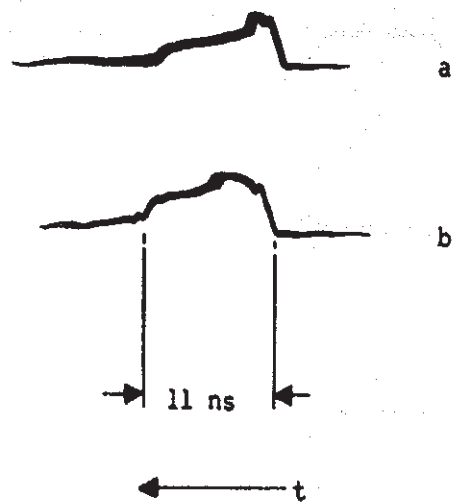


FIGURE 7
LOW LEVEL CALIBRATION PULSE

D-1368



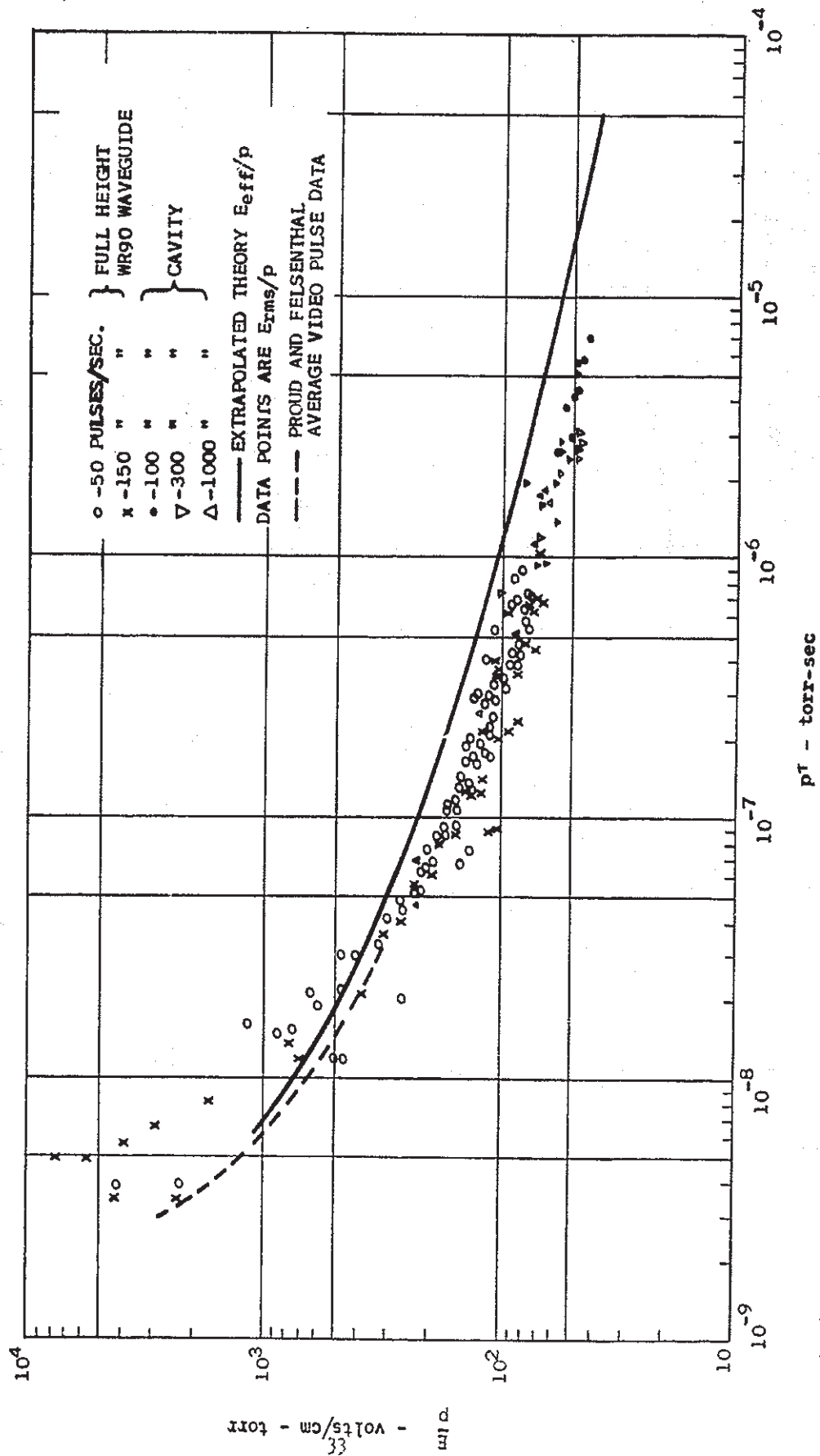
a. 40 mmHg AIR

b. 75 mmHg AIR

FIGURE 8
EXAMPLES OF PULSE DISTORTION BY BREAKDOWN

FIGURE 9

NORMALIZED PULSE BREAKDOWN IN NITROGEN



D-1386

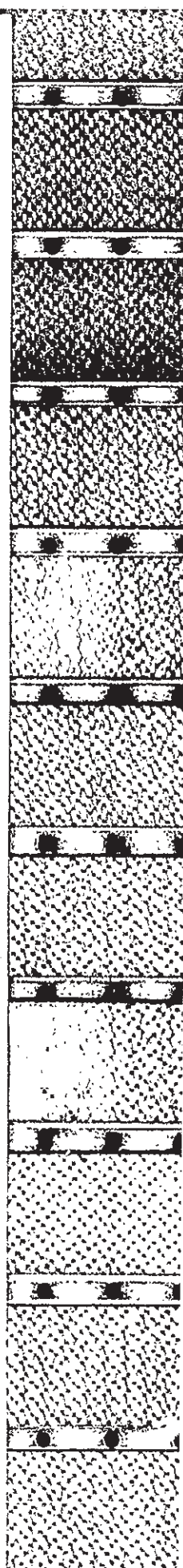
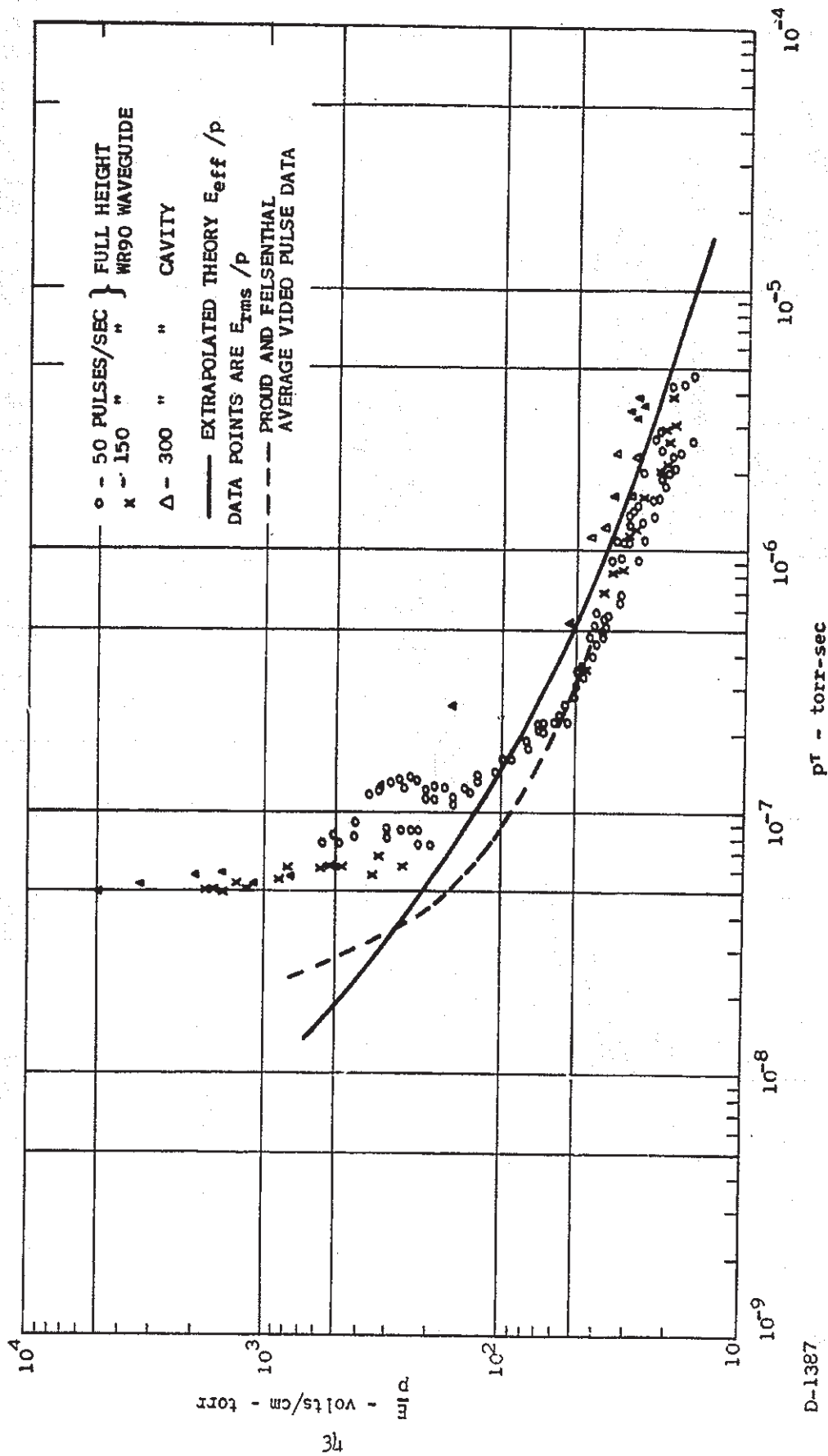


FIGURE 10

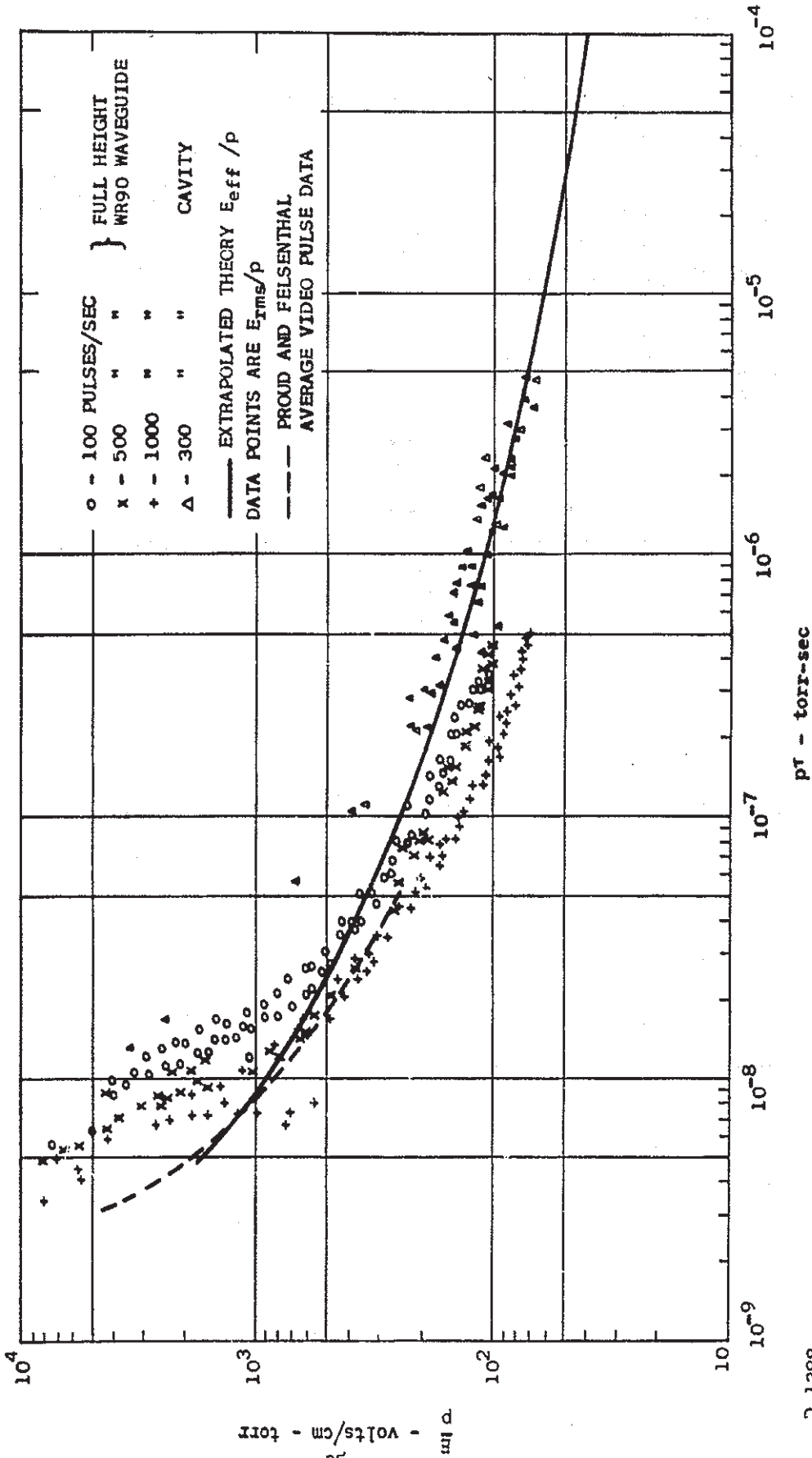
NORMALIZED PULSE BREAKDOWN IN HELIUM



D-1387

$p\tau$ - torr-sec

FIGURE 11
 NORMALIZED PULSE BREAKDOWN IN AIR



D-1388

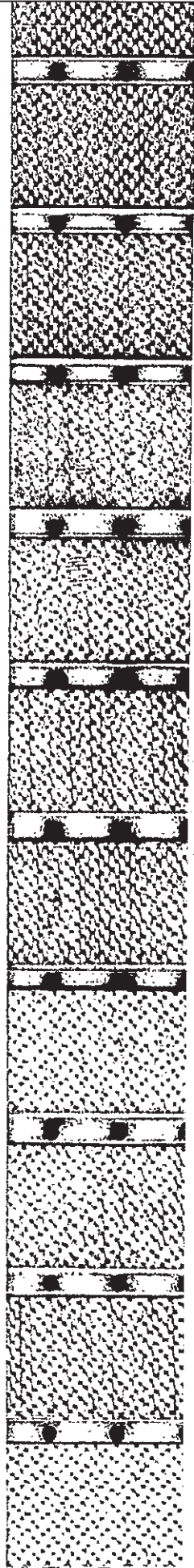
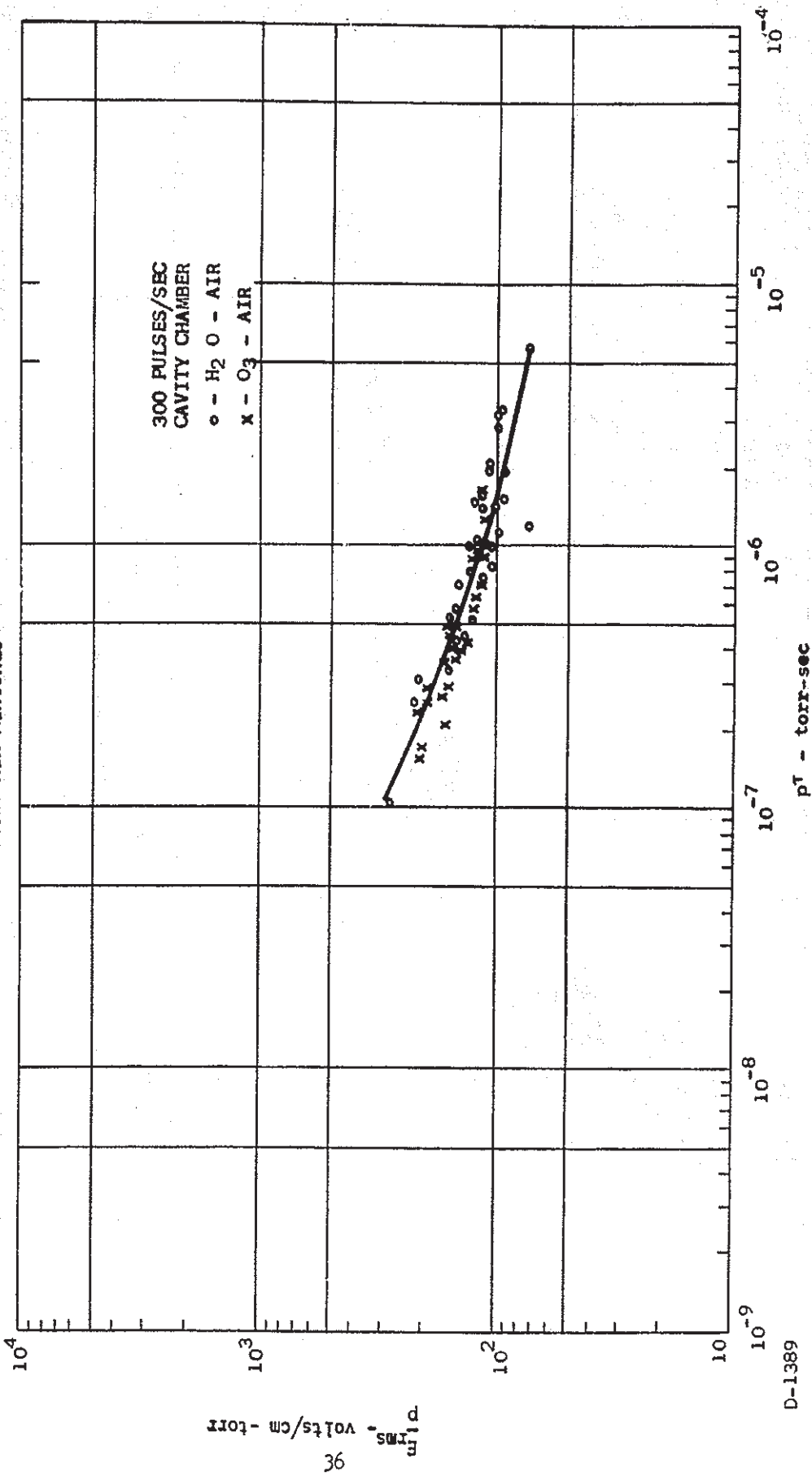


FIGURE 12
 NORMALIZED PULSE BREAKDOWN IN WATER-AIR AND
 OZONE-AIR MIXTURES



D-1389

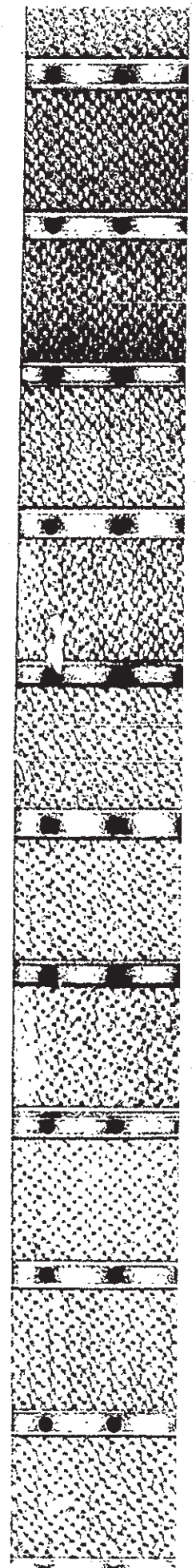
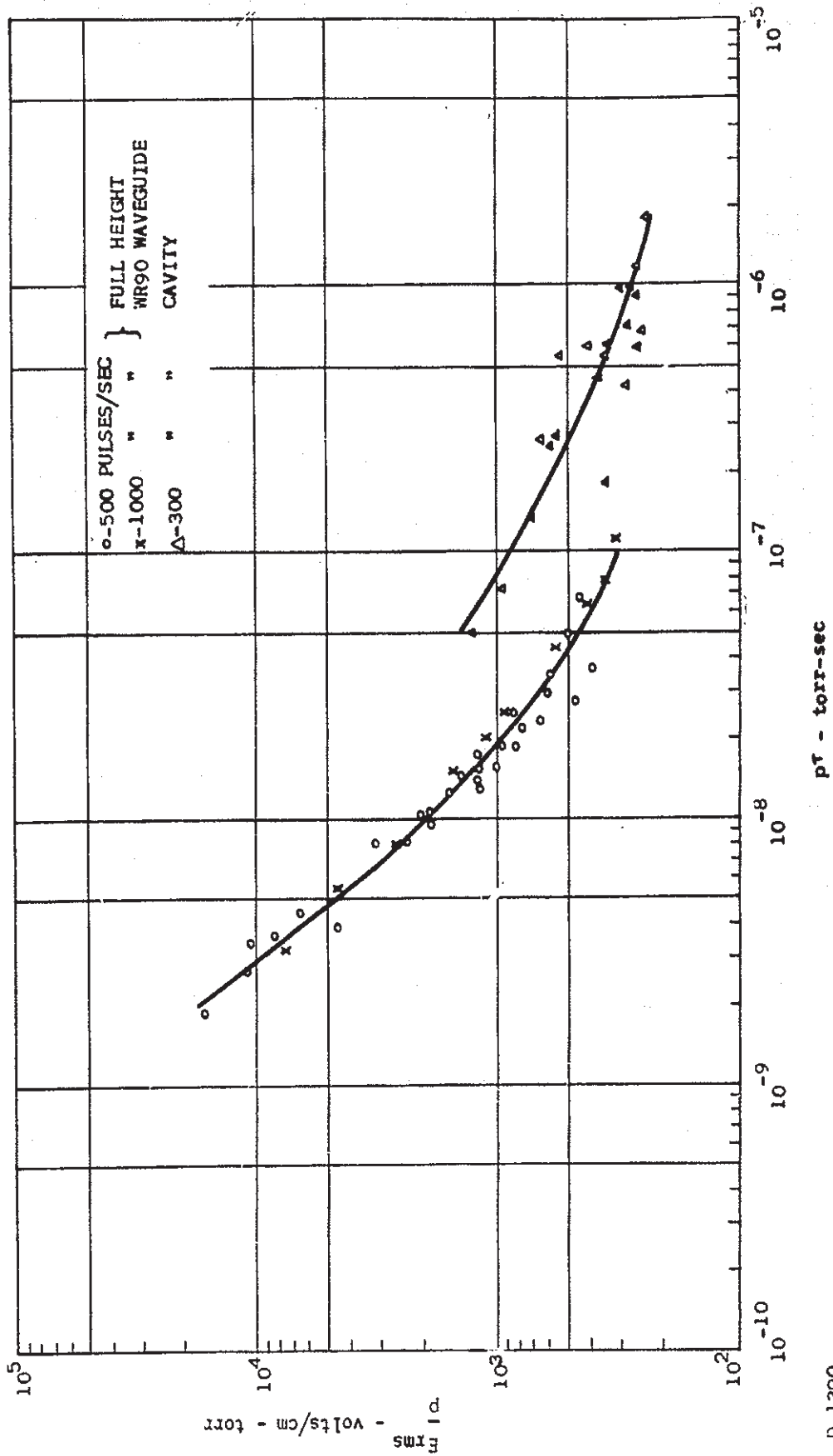


FIGURE 13
 NORMALIZED PULSE BREAKDOWN IN SULPHUR
 HEXAFLUORIDE



D-1390

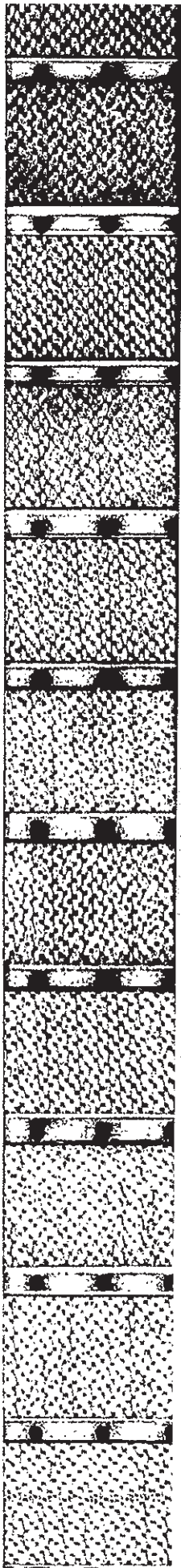
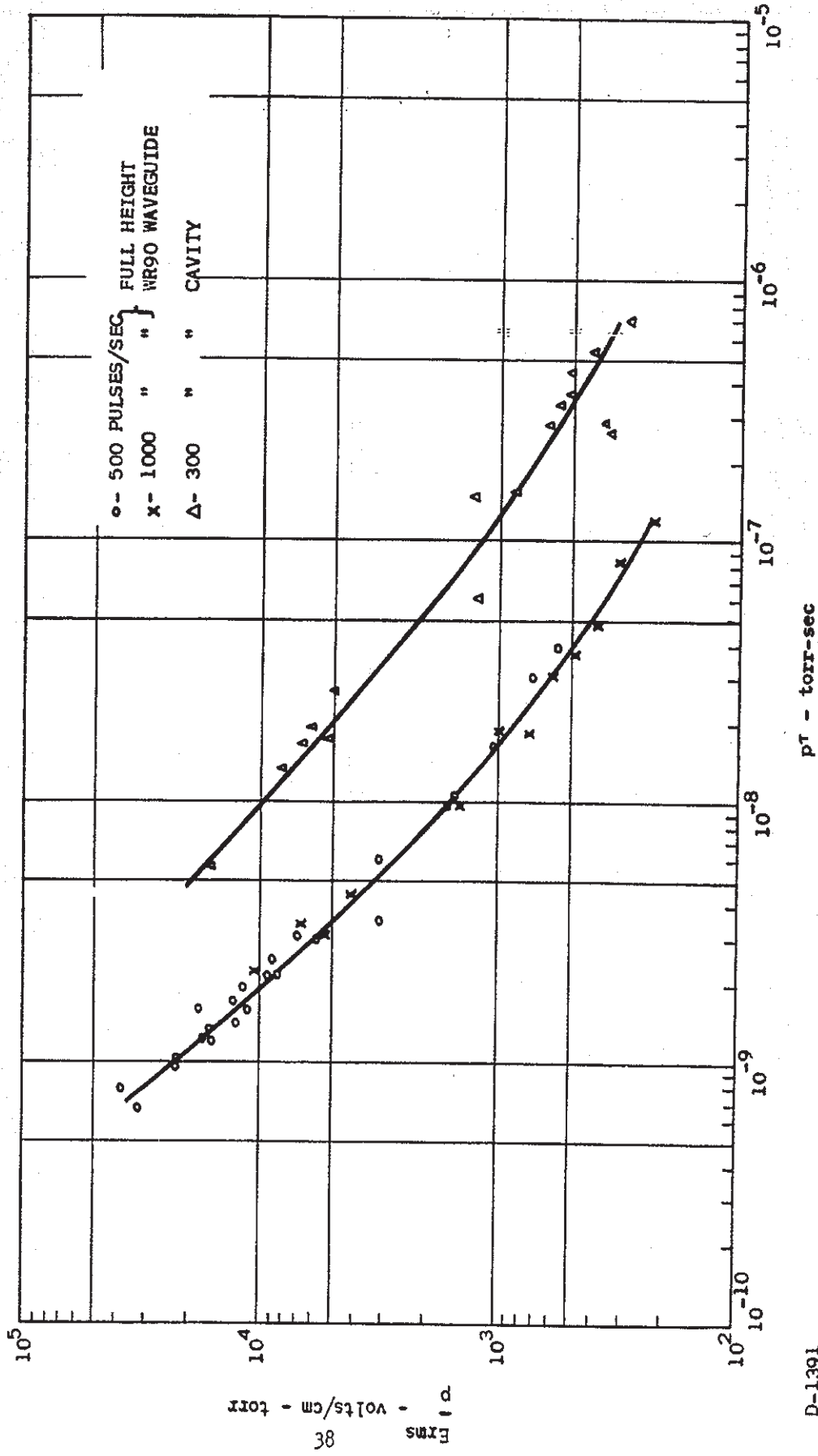


FIGURE 14

NORMALIZED PULSE BREAKDOWN IN FREON-12



D-1391

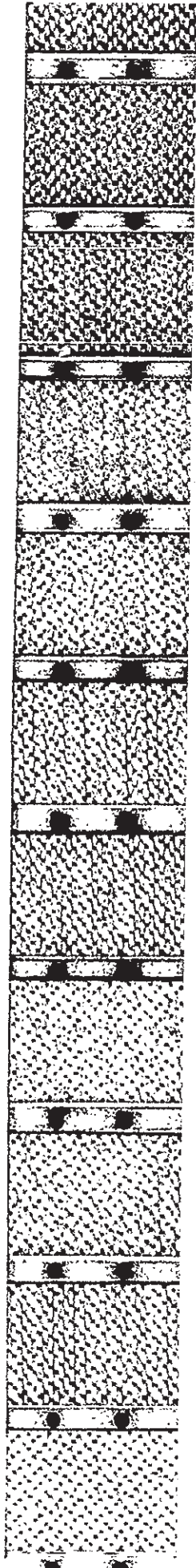


FIGURE 15

NORMALIZED PULSE BREAKDOWN IN FREON C-318

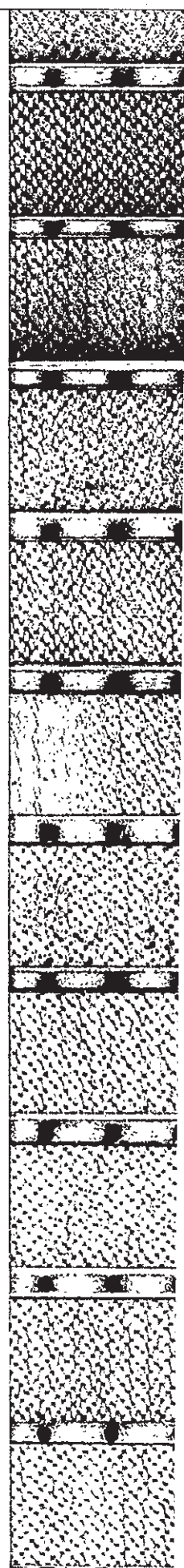
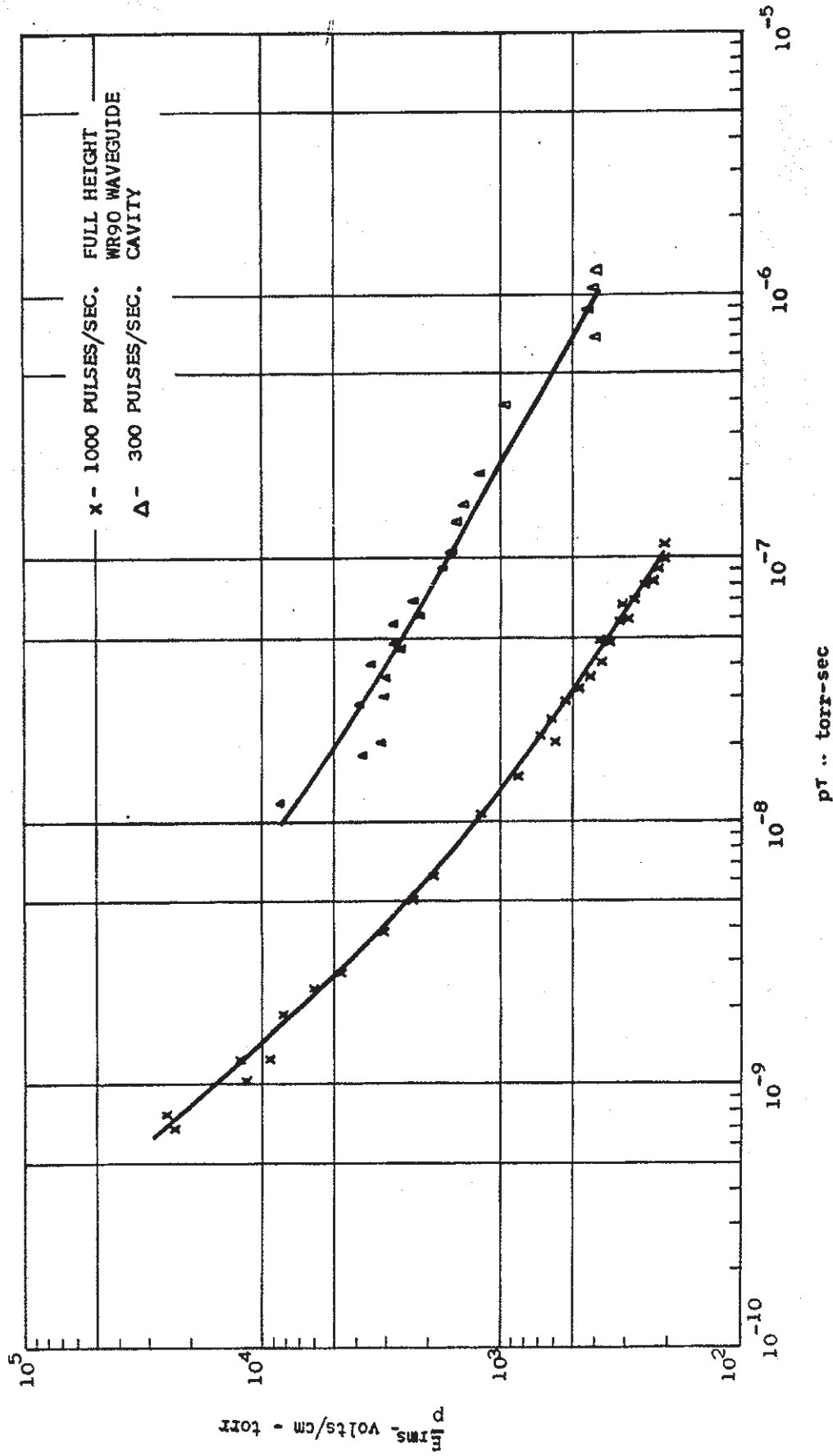
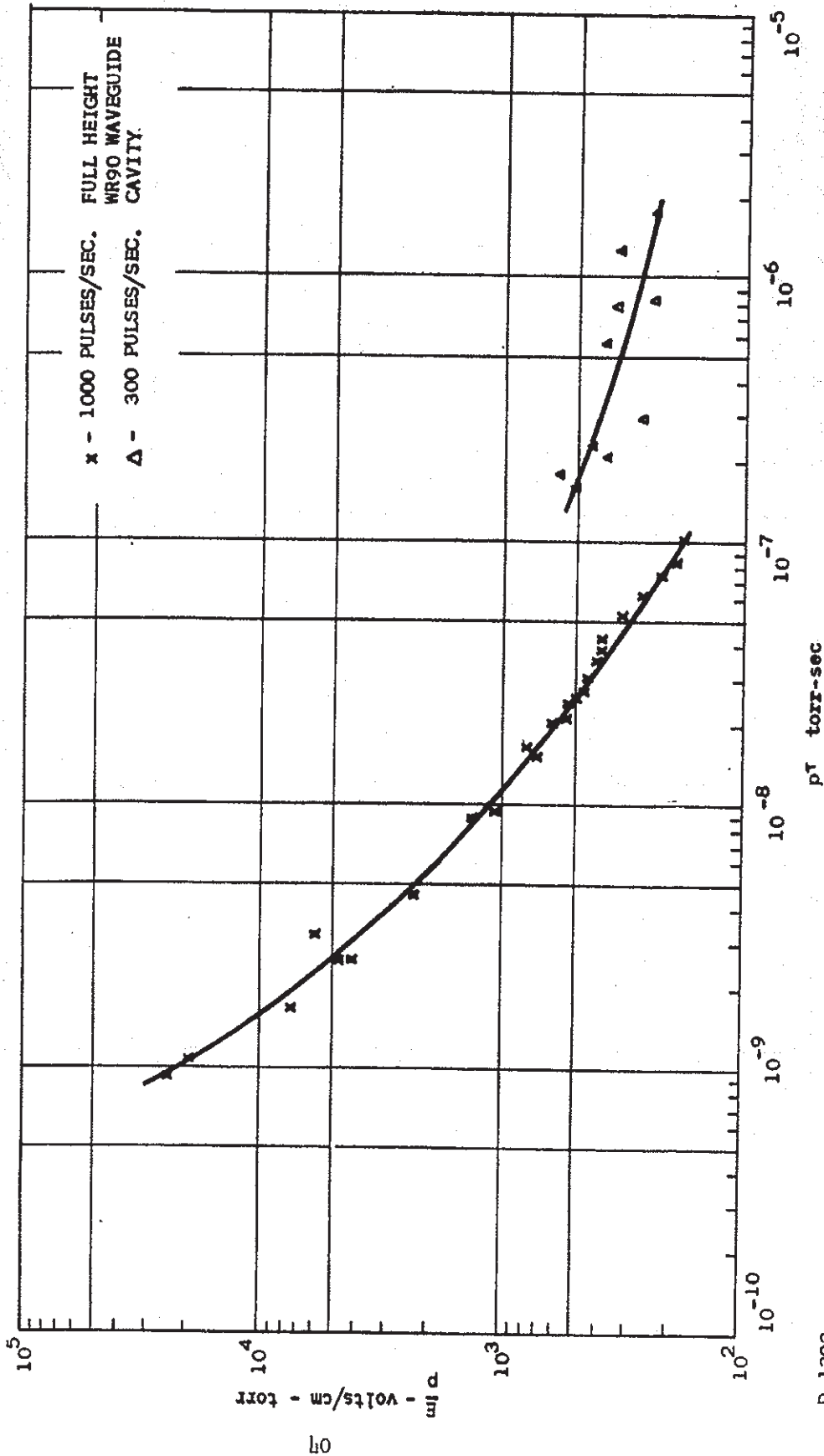


FIGURE 16

NORMALIZED PULSE BREAKDOWN IN FREON - 114



D-1393

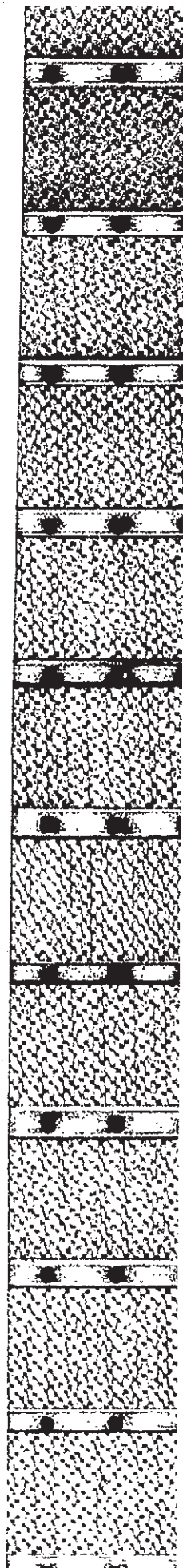
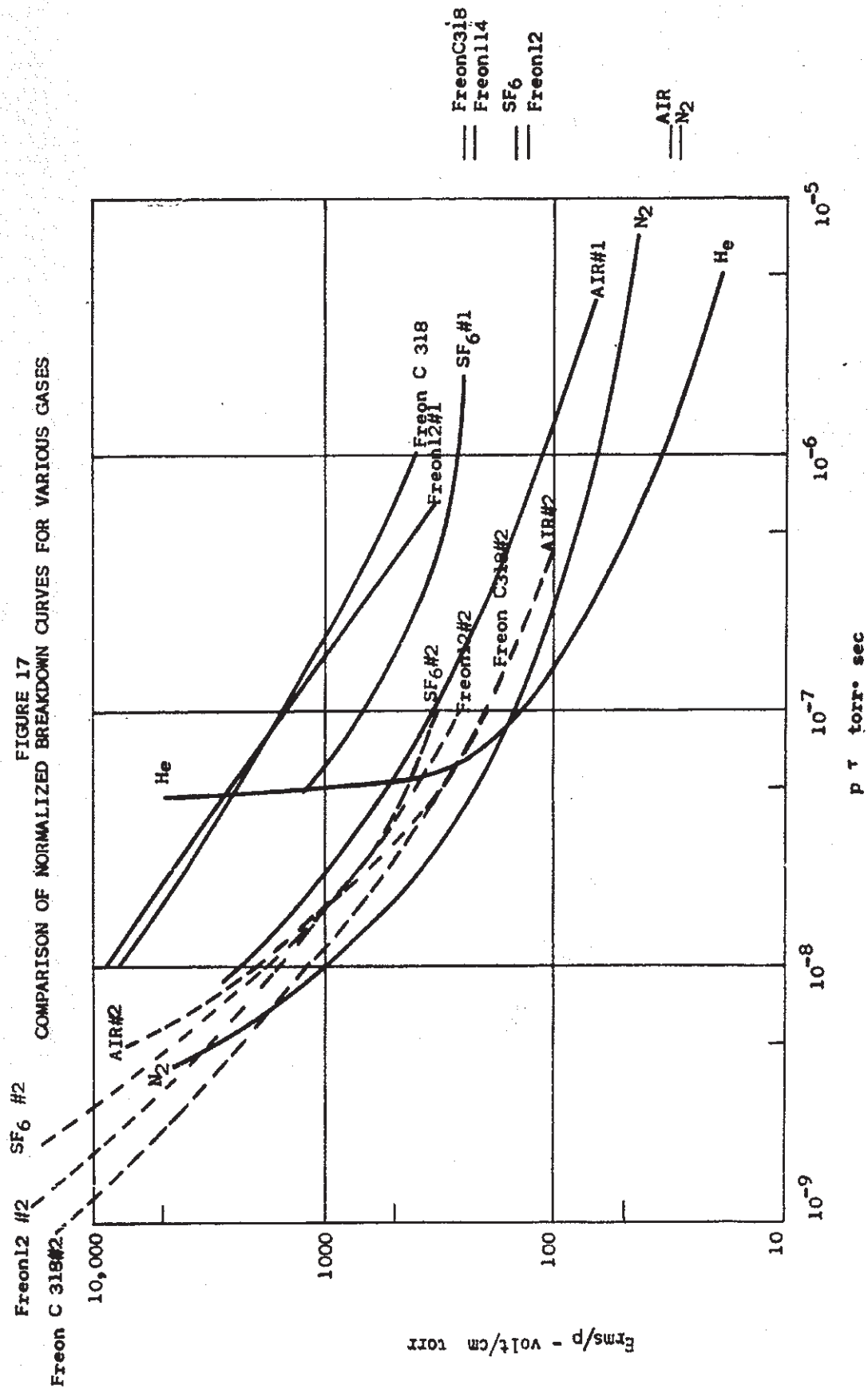
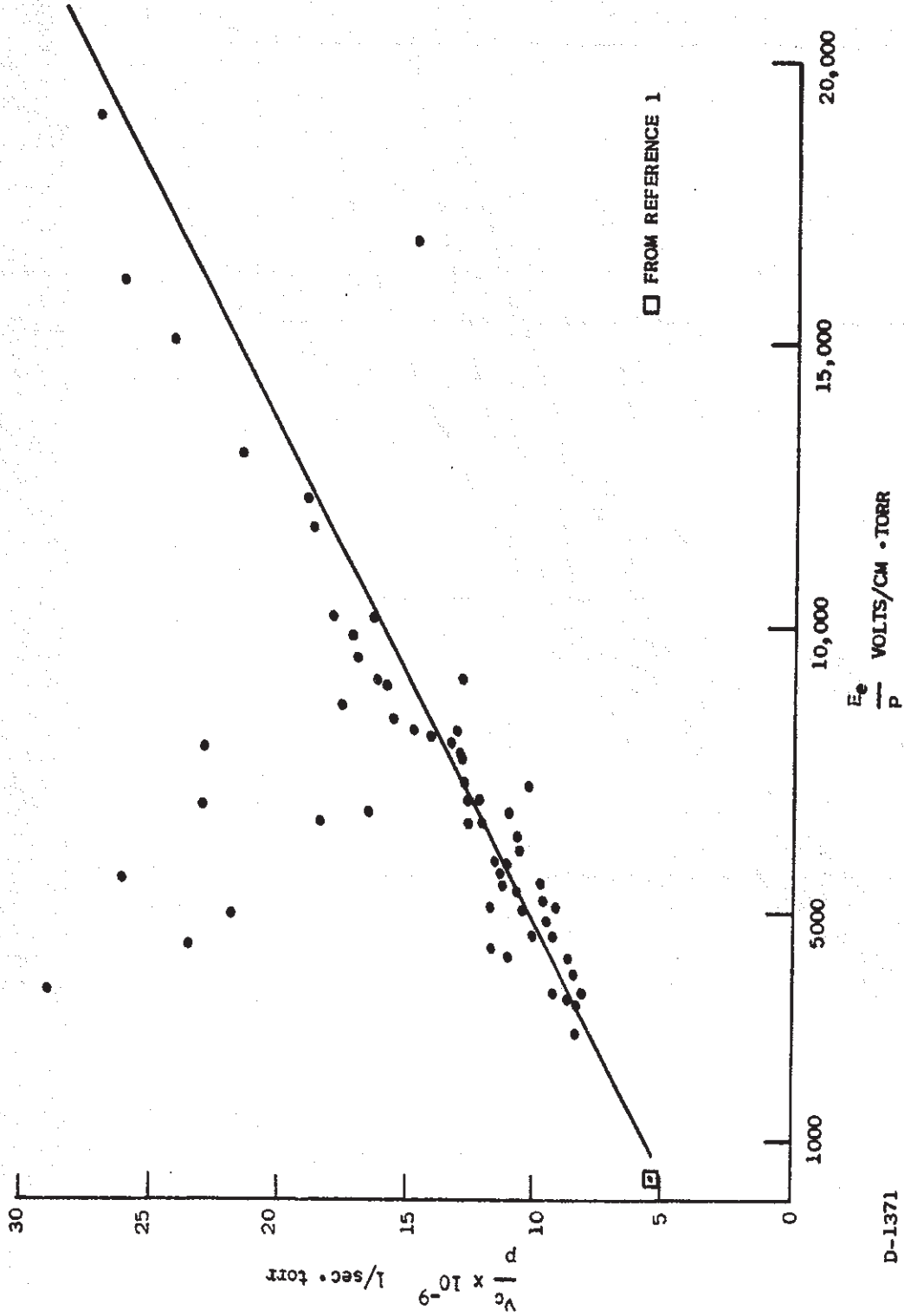


FIGURE 17
COMPARISON OF NORMALIZED BREAKDOWN CURVES FOR VARIOUS GASES



D-1407

FIGURE 18
ELECTRON COLLISION FREQUENCY IN AIR



D-1371

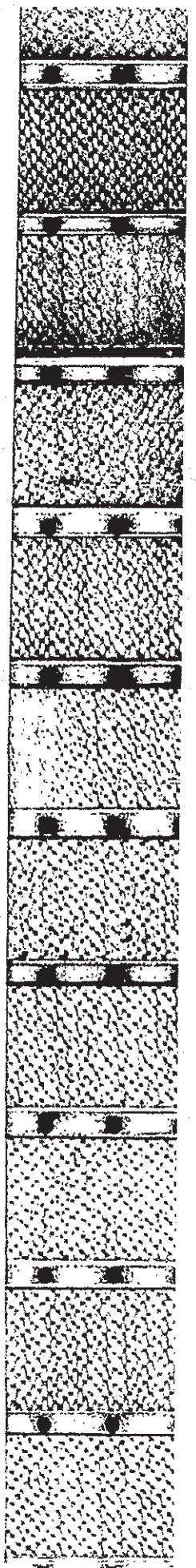
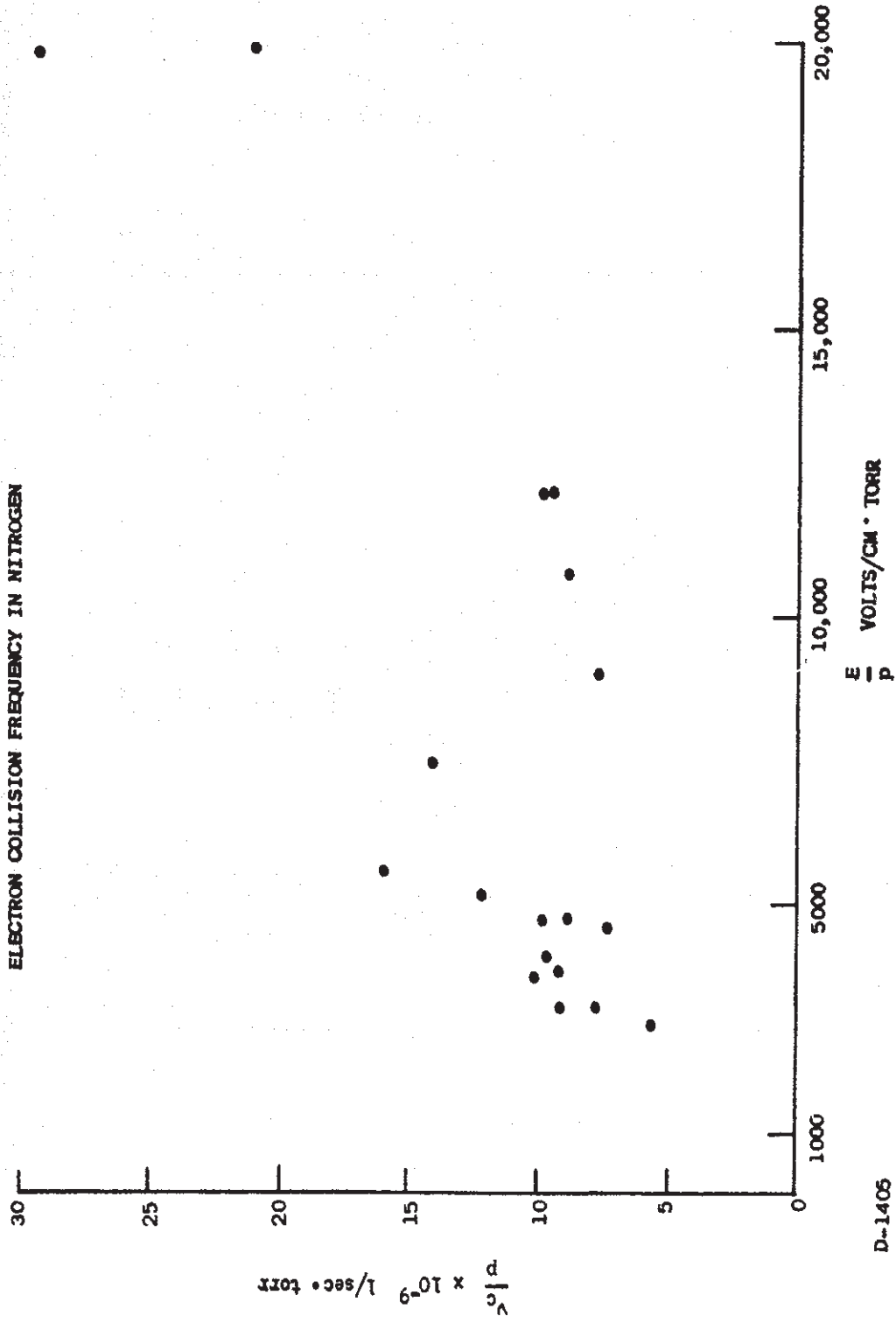


FIGURE 19
ELECTRON COLLISION FREQUENCY IN NITROGEN



D-1405

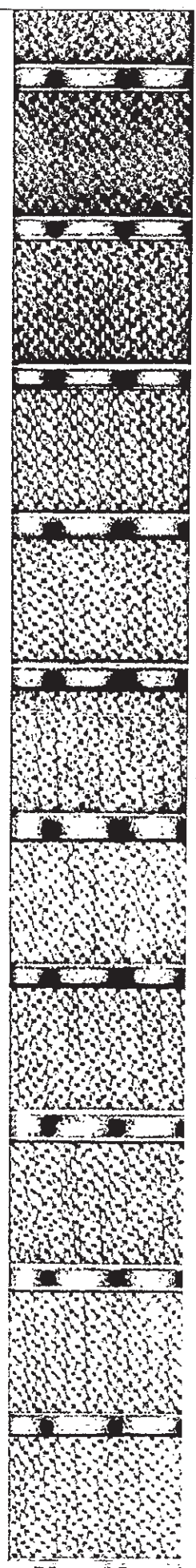
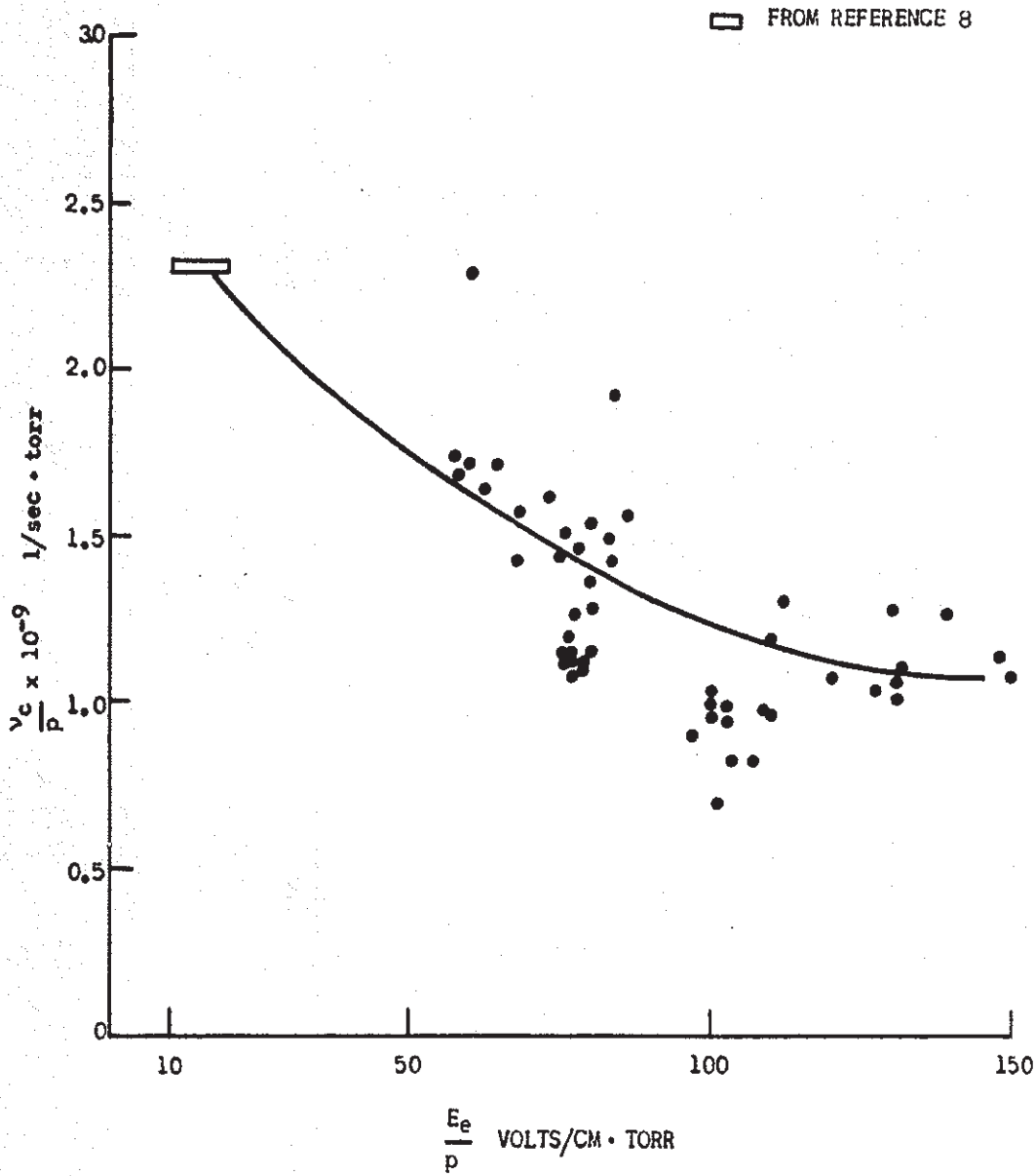


FIGURE 20

ELECTRON COLLISION FREQUENCY IN HELIUM



D-1406

hh